Catalysis Science & Technology

MINIREVIEW

View Article Online
View Journal | View Issue

Cite this: *Catal. Sci. Technol.*, 2017, 7, 4548

Photocatalytic pathway toward degradation of environmental pharmaceutical pollutants: structure, kinetics and mechanism approach

Samira Bagheri, Amin TermehYousefi and Trong-On Do *

During the last few years, the presence of pharmaceuticals in the aquatic environment, classified as so-called emerging contaminants, has attracted attention from the scientific community. Based on uptake mechanism and route administration of pharmaceuticals, they are expelled as a mixture of metabolites, neutral substance, or conjugated complex with an inactivating compound attached to the molecule. After usage, the expelled by-products are usually only partially metabolized and end up in the wastewater treatment plants. Large amounts of these substances are not destroyed by traditional sewage and wastewater treatment plants, thus eventually getting released into the environment. Their environmental existence has gained attention worldwide owing to related abnormal physiological processes in species reproduction, spurt incidences of cancer, enhancement of antibiotic-resistant bacteria and potential increment of hazardous chemical mixtures. Pharmaceutical pollution in the environment exists as a major issue for humans as well as the environment. These types of pollutants have been discovered in areas of low human population, such as the Antarctic. Although their influence, on both human health and the environment, is barely discernible, behavioral and physiological effects have already been detected in a number of species. In addition, there are several verified unfavorable impacts on human health such as presence of endocrine disruptors in low concentrations in the environment. Environmental pollution by pharmaceutical waste needs to be controlled through the quality use of medicines and quality sewage treatment. Through appropriate use of pharmaceuticals and suitable sewage systems, the environmental impact of pharmaceuticals may be reduced, without affecting the health danger gained through the intake of these medicines. Therefore, photocatalytic degradation of pharmaceutical pollution is a suitable method that should be reviewed and studied.

Received 11th March 2017,
Accepted 2nd August 2017

DOI: 10.1039/c7cy00468k

rsc.li/catalysis

Introduction

Over recent years, the use of antibiotics has considerably increased worldwide for the treatment of infectious diseases

Department of Chemical Engineering, Laval University, Québec City, Québec G1V 0A8, Canada. E-mail: Trong-On.Do@gch.ulaval.ca

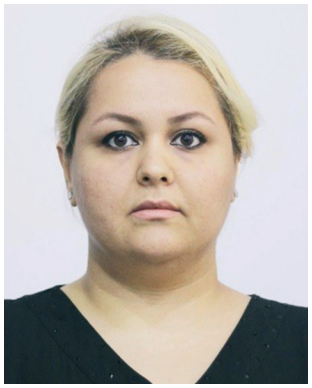

Samira Bagheri

Samira Bagheri is a visiting research fellow in the Department of Chemical Engineering at Laval University, Canada. Samira's main research interests include carbon nanomaterials, such as carbon nanotubes and graphene nanosheets, metal oxide nanocomposites, and advanced smart nanohybrids has focused on the application of such materials in photoelectrochemical hydrogen production and environmental pollution management.

Amin TermehYousefi

Amin TermehYousefi is a visiting research fellow in the Department of Chemical Engineering at Laval University, Canada. Amin's research interests include carbon nanomaterials, such as graphene nanoribbons, and fabrication of solar-energy-driven photocatalysts based on carbon nanomaterials.

and agricultural productivity.[1] Keiji Fukuda once said that "the world without antibiotics would look very different to the world we live in now". However, with the deliberate release of antibiotics to the environment and lack of effective treatments of antibiotic wastewater, antibiotic pollution poses a serious environmental threat to both aquatic and terrestrial ecosystems. Generally, antibiotics are a type of antimicrobial used for medical applications in humans and animals and are also added to animal feeds to prevent diseases and enhance growth.[2] Based on their pharmacological properties, the main categories of antibiotics include aminoglycoside, β-lactam, glycopeptide, macrolide, quinolone, sulfonamides, and tetracycline (TC).[3]

Sulfonamides, polar, photo- and thermally stable substances that are soluble in water,[4] are the most frequently used antibiotic in human medicine as they have a high migration ability in the environment.[5] Subsequently, the second most frequent antibiotic used is tetracycline (TCs). In many countries like the USA, China and India, tetracycline (TC) is reported as the most widely used antibiotic[6] in animal feed.[7] Tetracycline antibiotics, (TCs) especially tetracycline (TC), oxytetracycline (OTC), and chlortetracycline (CTC), have been widely used in animal medicine and aquaculture activities due to their ability to present a threat to biota, disrupt indigenous microbial populations, and disseminate antibiotic-resistant genes among microorganisms.[8,9] Thus, by-products of tetracycline antibiotics are hazardous to humankind.

Non-steroidal anti-inflammatory drugs (NSAIDs) are some of the most frequently detected groups of pharmaceuticals in environmental samples, as they are one of the most widely available drugs in the world.[10,11] The main characteristic of the NSAID group is the carboxylic aryl acid moiety that is responsible for their acidic properties.[12] Ibuprofen (IBP) belongs to this family of medicines; it is an analgesic drug mainly used for treatment of myoskeletal injuries and fever. IBP has been reported to have a toxic impact on microbial communities.[13,14] Carbamazepine (CBZ) is a neutral anticonvulsant pharmaceutical used primarily in cases of epilepsy and bipolar disorder. CBZ has been reported to be present in effluents of wastewater treatment plants, and toxicity studies have concluded that CBZ is associated with early maturation and chronic toxicity in ceriodaphnids.[1,15] Therefore, the removal of pharmaceutical compounds up to an allowable permissible limit from the wastewater is essential before discharge into the drainage system.[16,17] The presence of these pharmaceutical pollutants may cause serious threats to the environment. The photocatalytic decomposition of pharmaceuticals has been a promising degradation method.[18] Semiconductor photocatalysis is capable of splitting water into hydrogen and oxygen and degrading organic pollutants under sunlight illumination. Since the driving force of semiconductor photocatalysis comes from sustainable and "green" solar energy, it is regarded as one of the most promising strategies to address worldwide energy and environmental issues.[19] TiO_2 is widely investigated due to its high photocatalytic activity, non-toxicity, long-term stability and relatively low price.[20,21] However, it has shortcomings such as fast electron–hole recombination and low quantum yield, which lead to a low effectiveness and high cost. Therefore, substantial research efforts have aimed to modify TiO_2 materials to expand the band gap to slow down electron–hole recombination rate.[22,23] Photocatalyst modification methods include doping metal and nonmetal ions and the creation of a heterojunction with other semiconductors.[24] Another approach to improve photocatalytic activity of TiO_2 is to incorporate nanostructured carbon materials.[25] Sioi *et al.* have investigated the decolorization of pharmaceutical wastewater using TiO_2 P25 as a heterogeneous photocatalyst, revealing that photocatalytic oxidation is a powerful alternative technology for degradation of hematoxylin.[26,27] Their results also show that the performance of P25 nanoparticles do not decrease after reuse, and thus, these nanoparticles are suitable for practical wastewater treatment.[28]

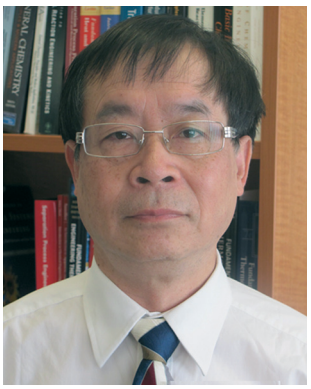

Trong-On Do

Trong-On Do is a full-time professor in the Department of Chemical Engineering at Laval University, Canada. He received his MSc in 1986 and Ph.D. in 1989 from the University of P. and M. Curie (Paris 6, France). After some time at Brunel University (UK) and the French Catalysis Institute (France), he moved to Laval University in 1990. He then spent two years (1997–1999) in Profs. Hashimoto/Fujishima's group at Kanagawa Academy of Science and Technology under the Japanese STA Fellowship Award before re-joining Laval University as a professor associated with the NSERC Industrial chair. He has published over 140 papers and review articles in refereed journals and holds 5 international patents. He is the recipient of the 2014/2015 Canadian Catalysis Lectureship Award (CCLA).

1.0 Environmental persistent pharmaceutical pollutants (EPPPs): organic pollutants

Among other things, microbial populations pose a potential threat of transfer of the genes favoring survival.[2] These persistence genes are often resistant and can barely be eliminated, even without the antibiotic pressure.[3] Therefore, essential action to eliminate antibiotic residues in wastewater should be taken. Various treatment processes such as photocatalytic degradation,[4,5] ultrasonic induced processes,[8,9] electro-coagulation,[29] advanced biological methods with COD removal of up to 80%,[30] adsorption[8] and photoperoxi-

coagulation[30] have been studied for the removal and degradation of recalcitrant contaminants like TC in the aqueous phase.

1.1 Analgesics and non-steroidal anti-inflammatory drugs

These days, anthropogenic pollution has evoked serious environmental issues worldwide, concerning the relationship between humans and the environment if no appropriate precautions are taken.[6,7] One of the major problems is the presence of pharmaceutical pollutants in natural water systems and groundwater,[31,32] which usually exist in concentrations of parts per billion (ppm) or even parts per million (ppb). Pollutants reach water effluents through discharge from industries and secretion of non-metabolized drugs by humans or animals through urine and feces. Among these pollutants, non-steroidal anti-inflammatory drugs (NSAIDs) such as diclofenac (DCF) and fluoxetine are common.

Diclofenac, the most prescribe non-steroidal anti-inflammatory drug (NSAID), is usually found in hospitals and in sewage water systems and septic tanks, and it is excreted unmetabolized and released in the aquatic environment because of the inability of conventional wastewater treatment plants to degrade this type of contaminant, causing various problems.[33,34] According to Lindholm-Lehto and co-workers, diclofenac is detected in concentrations ranging from ng L^{-1} to μg L^{-1} in surface water as only it is only moderately removed in wastewater treatment.[35] Such levels are a cause of concern as DCF concentration above 5 μg L^{-1} can cause renal lesion and gill alteration in rainbow trout.[36] Besides, studies have reported that DCF may also be the cause of the tremendous increase in renal failure in countries such as Bangladesh, Pakistan, Nepal, and India.[36–38] Another study on diclofenac reports that its residues can prompt structural problems in the kidney and intestine and alter functional genes that are associated with the main process of controlling metabolism.[39] Thus, DCF has recently been added to the pollutant "watch list" compiled by the European Union. Fluoxetine is a selective serotonin reuptake inhibitor, used for the treatment of clinical depression, obsessive–compulsive disorder, and bulimia. It is one of the most often prescribed drugs in the United States. According to literature data, FXT detected in wastewater treatment effluent in high concentrations (μg L^{-1})[40] is also considered as a hazardous pollutant to the aquatic environment and is toxic to neonate sea species such as *Ceriodaphnia dubia*, with average lethal concentrations being 0.51 mg L^{-1}.[41,42] Hence, in order to prevent long-term effects, it is crucial to develop efficacious technologies to eliminate and break down such compounds to prevent their discharge into the environment. Besides, it is essential that such technologies are effective, environmentally friendly and economically viable.[43,44]

1.2 Antineoplastics

Antineoplastics are agents that traverse the whole body and kill cancer cells. The most common effect of antineoplastics is bone marrow depression. Hydroxyapatite is a calcium phosphate ($Ca_{10}(PO_4)(OH)_2$,HAp) mainly used in biomedicine; as the main component of human bones and teeth, it is highly biocompatible.[45] HAp can also be employed for environment remediation; its capacity to adsorb heavy metals has been investigated.[46] More recently, it has been shown that HAp has photocatalytic properties; moreover, when combined with TiO_2, very powerful photocatalysts can be synthesized due to a synergistic effect between the two compounds.[47,48] Ti-doped HAp is also reported to have photocatalytic activity.[45] HAp-based materials have been tested in liquids for photodegradation of organic molecules and/or dyes (*i.e.* methylene blue, calmagite);[47,48] however, they have never been utilized to degrade pharmaceutical pollutants.

Most HAp-based materials used today are prepared synthetically by chemical reaction between calcium and phosphorus. However, HAp can also be extracted naturally from animal/fish bones and/or minerals.[49] Previous work done by our group showed that HAp can be extracted from cod fish bones through a simple calcination process; the resulting materials showed biocompatibility.[50] Moreover, with the bones treatment in appropriate solutions, HAp-based materials with photocatalytic properties could be obtained. A full physical and structural characterisation of these materials were previously performed, while their photocatalytic properties were only tested for degradation of blue methylene.[51] The objective of this work is to use HAp-based materials of marine origin to photodegrade two micropollutants – DCF and FXT. As HAp-based photocatalysts have never been employed to degrade this kind of molecules, our aim is to verify if these photocatalysts are suitable for this application.

1.3 Effects of EPPPs on human health

Pharmaceuticals can tremendously improve human health and quality of life when used to treat contagious diseases. However, misuse of drugs, especially antibiotics, impacts the environment and human health. Notable changes in sex ratio and fecundity of *Daphnia magna* were reported on exposure to pollutants such as sulfamethoxazole, trimethoprim, and triclosan.[52] Also, experiments on male rats showed hypoandrogenization and decrease in desire and sexual motivation on exposure to cimetidine.[53] Thus, continuous release and perfusion of these pharmaceutical pollutants in water environments and organisms can seriously harm the environment by causing genetic exchange and activating drug resistant bacteria.[54,55] Furthermore, most pollutants, even in low concentrations may lead to serious risk to the ecosystem and human health.[56]

According to the World Health Organization, these pollutants are usually introduced into the sewage system through excretion of unmetabolized compounds after medical use or through improper disposal[57,58] in wastewater treatment plants (WWTPs). However, conventional WWTPs are not designed to treat pharmaceutical pollutants present in trace amounts, rendering the WWTPs ineffective in their

removal.[59,60] Consequently, pollutants reach the aquatic system and accumulate in surface and ground water,[61] soil, and sediments[62] and even in drinking and tap water.[63] Although usually pharmaceuticals do not present acute toxic effects on aquatic organisms due to their low concentrations, in the range of ng to μg per liter, concerns have been raised about chronic exposure, as they are slightly persistent pollutants continuously released into the environment[48,60,63] in biologically active levels.[64] Thus, elimination of emerging pollutants from wastewater is favorable and essential for quality of life and environmental protection. For these reasons, diverse efforts to explore promising technologies for degrading pharmaceuticals from wastewater, such as reverse osmosis, solar/advanced oxidation processes (AOPs) and adsorption on activated carbon, have been studied.

2.0 Conventional methods for pharmaceutical waste treatment

2.1 Reverse osmosis

Photocatalytic treatment by reverse osmosis has drawn tremendous attention due to its distinct efficiency and low cost in eliminating organic contaminants.[65] A study has been conducted focusing on key transport mechanisms of a combined membrane bioreactor (MBR) through commercially available NF/RO membranes.[66] Results show that elimination of organic contaminants by NF/RO membrane filtration complement well with MBR treatment, which tremendously enhances the removal of organic contaminants by 96%. Thus, MBR treatment with NF/RO can efficaciously eliminate hydrophobic and readily biodegradable hydrophilic organic contaminants. The remaining hydrophilic and biologically emerging contaminants are shown to be effectively eliminated by UV oxidation.

Martínez *et al.*, (2013)[47] have also conducted experiments on membrane separation and heterogeneous photocatalytic oxidation processes for treatment of emerging pharmaceutical pollutants. In this system, two different membranes (one for nanofiltration and the other for reverse osmosis) are studied as selective barriers to eliminate pharmaceutical pollutants. The efficiency of heterogeneous photocatalytic methods by semiconductor Degussa P-25 TiO_2 and hematite iron oxide supported on a mesoporous silica support (Fe_2O_3/SBA-15) is observed. In general, it can be concluded that reverse osmosis can be very practical for removing pollutants, but it requires additional treatment.

2.2 Chemical and biological degradation

Chemical and biological degradation are traditional sewage treatment comprising four removal stages. They are preliminary treatment, primary treatment, secondary treatment and advanced wastewater treatment. Preliminary treatment is used in the removal of coarse and large solids, minimizing oils, fats, grease, sand, and grit, by mechanical means such as filtration and bar screening. Primary treatment involves separation of organic suspended solids. This process enables effective enhancement of operation and maintenance of following treatment units. Secondary treatment (aeration stage) serves to break down organic content of the sewage *via* microorganisms. Lastly, the 'almost' treated wastewater is passed through a settling tank. This step employs bacteria for specific contaminants that cannot be removed by secondary treatment to produce clean filtered water. Therefore, biological and physicochemical processes can be useful for the removal of pharmaceutical contaminants released into streams, rivers or lakes, as they are may be eliminated by adsorption onto suspended solids, during aerobic and anaerobic degradation, or chemical (abiotic) degradation by hydrolysis.[67,68] Investigation of the elimination of organic contaminants such as antibiotics, proteins, and lipid regulating anti-inflammatory drugs by chemical and biological degradation has reported a removal efficiencies of less than 20%.[68] In addition, biotic elimination processes have been studied by Yang and co-workers, where sulfonamide was biodegraded in the presence of activated sludge with and without addition of NaN_3 biocide.[34] Promising results in the removal of trace antibiotics from wastewater have been noted.

2.3 Advanced oxidation process (Fenton-like reactions)

Approaches such as advanced oxidation processes (AOPs) are gaining importance as promising methods to treat emerging pharmaceutical pollutants in wastewater.[69] This is because AOPs are considered to be particularly effective in the treatment of toxic and non-biodegradable persistent organic substances[70–72] due to their potential oxidizing properties. Mainly, AOPs can be classified under ozonation, sonolysis, homogeneous wet oxidation, ultraviolet irradiation, Fenton process or heterogeneous photocatalysis using semiconductors, radiolysis and a number of electrical and electrochemical methods.[72] Among these techniques, photocatalysis by Fenton process is identified to have some advantages such as easy setup and operation at room temperatures. Besides, it is known as an effective system for mineralization of many pollutants through the production of $^{\bullet}OH$ and $O_2^{-\bullet}$ radicals.[73,74] Catalysts of titanium dioxide in oxidation have widely known to degrade organic pollutants as they possess good stability and are environmentally friendly. Moreover, generated holes (h^+) and electrons (e^-) from the illumination of TiO_2 with light ($\lambda < 420$ nm) can effectively react with adsorptive water molecules to produce active radicals,[75] aiding in increased degradation efficiency.

In AOPs, hydroxyl radicals ($^{\bullet}OH$) are induced by photoinduced charge separation of electrons and holes. These active species react with water or oxygen to form reactive oxygen species (ROS), which can mineralize most resistant organic substances and break them down into somewhat less-persistent organic by-products, known as "green" chemicals, carbon dioxide (CO_2) and water (H_2O).[74] Besides, AOP involving heterogeneous photocatalysis using a ultraviolet (UV) light source or solar irradiation has been known to be

effective for the degradation of several types of persistent pollutants[76] as ultraviolet light ($\lambda < 400$ nm) can act as an energy source and TiO_2 serves as a semiconductor photocatalyst.[77,78]

Długosz *et al.* (2015)[79] reported that using AOPs with a photocatalyst showed a corresponding decrease in total organic pollutant (TOP) content and degradation efficacy with respect to antibiotics such as ampicillin, cloxacillin, amoxicillin,[79] tetracycline[80] and sulfamethoxazole.[81] Neamțu and colleagues (2014)[157] investigated the photodegradation of eight micro-pollutants, namely benzotriazole, atenolol, clarithromycin, metformin, methylbenzotriazole, metoprolol, gabapentin and primidone, in lake water and wastewater effluent by the photo-Fenton process and hydrogen peroxide (UV_{254}/H_2O_2) under UV light irradiation (254 nm). In lake water, the removal efficiency was approximately 55%, whereas it was about 30% in wastewater effluent. In addition, evaluation of performances of three different techniques of AOPs, namely the photo-Fenton process ($Fe/H_2O_2/UV$) (as an example of a liquid–liquid reaction), the TiO_2 photocatalytic oxidation process (TiO_2/UV) (a solid–liquid reaction), and the combined ozone and hydrogen peroxide (O_3/H_2O_2) oxidation process (a gas–liquid reaction), for the removal of pharmaceuticals was conducted, whereby effects of aqueous matrices were taken into account. The effects of Fenton process on elementary pollutant degradation improved because of the presence of CESs having additional iron ions, while the photoreduction reaction was hampered by the complex-forming reaction. This was further confirmed by Tokumura *et al.*,[83] who found that CESs could improve degradation of emerging contaminants not only *via* scavenger effects and light scattering (photo-Fenton process), but also by adsorption on active sites on the surface of TiO_2 photocatalyst.[84]

2.4 Solar-driven photocatalyst

Today, solar driven photocatalysts are gaining interest because they are able to eliminate harmful or non-biodegradable pollutants from the environment. They are pertinent from two perspectives: (a) photocatalytic process is the ultimate solution for elimination of pollutants in natural aquatic systems[5] and (b) they are established as an emerging green technology for wastewater treatment.[2] Thus, it significantly plays a relevant role in assisting dissolved organic matter (DOM) and humic substances (HS). This technique involves "*in situ*" generation of active oxidizing species under solar irradiation in the presence of a catalyst, titanium dioxide, as shown in Fig. 1.

Several studies have been conducted in the past decade on the uses of these processes to treat a large range of pollutants using sunlight.[65–68] Their function as a preliminary treatment aiding biocompatibility of hazardous, non-biodegradable emerging effluents has earned considerable attention lately.[86–88] Therefore, using solar driven photocatalysis as a pre-treatment might be desirable to eliminate emerging contaminants from effluents of wastewater treatment plants. In fact, some reviews have investigated the applicability of solar

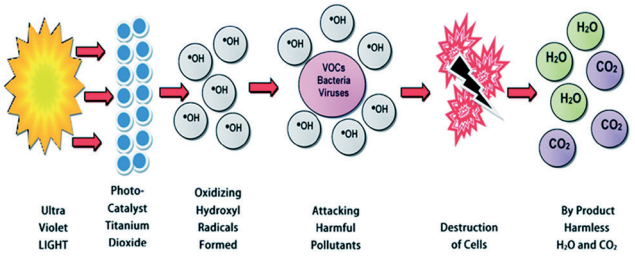

Fig. 1 Solar-driven photocatalysts in elimination series of emerging pollutants in natural aquatic systems.[85]

driven photocatalysis as a tertiary treatment to remove emerging pollutants[89–91] of considerably low concentrations (*ca.* 5 μg l^{-1}) in effluents from wastewater treatment plants[87,88] with satisfactory results. Nonetheless, researchers reported on the treatment of various pollutants such as dyes[92,93] or even some pharmaceuticals[94] by photocatalytic reactors with membrane cells are able to discrete and recirculate of TiO_2 catalysts to the photoreactor, which shows an increase in the overall performance of the process, which proved the successful results in eliminating aromatic sulfonic acids,[85] phenols, as well as azo[95] and cationic dyes[96] dyes by SBO-mediated photodegradation, can be done in complement to bigger scale direct sunlight photo-remediation of a wide number of pollutants.[76]

Photocatalysis has emerged as a green technology for the complete mineralization of hazardous organic chemicals to water, carbon dioxide, and simple mineral acids.[97–99] This reaction is light-induced and is enhanced by the presence of a catalyst. An ideal photocatalyst should be nontoxic, inexpensive, stable, easily available and highly photoactive.[100] This solar-driven photocatalysis has many advantages over other methods, such as low cost, reusability, complete degradation and eco-friendly.[101–103] TiO_2 has emerged as the best photocatalyst for degradation under UV light, because it is easy to prepare and recyclable, tolerates both acidic and alkaline solutions, is stable and does not require any strong oxidizing agent.[104,105] In recent years, semiconductor photocatalysis has shown great potential as cost effective, environment friendly and sustainable treatment technology with zero waste discharge.[106–109] Photocatalysis involves removal of water contaminants that are chemically stable and resistant to biodegradation.[110] The method offers an advantage over usual wastewater treatment techniques such as activated carbon adsorption, chemical oxidation, biological treatment and membrane separation.[111] Activated carbon adsorption involves phase transfer of pollutants without decomposition. This incomplete removal process further increases pollution load on the environment.[112] Chemical oxidation is also a cause of incomplete mineralization of organic substances with the generation of undesirable toxic byproduct. Biological treatment faces the crises of sludge removal, very slow reaction rate and control of appropriate process conditions (microbial growth condition). The disadvantages of retentive components, severe membrane fouling, and costly setup

great impact membrane process. In this context, photocatalytic processes offer a number of advantages for the removal of pollutants from water, complete mineralization, use of low-cost catalyst system and comparatively hassle-free arrangement.[110,113,114]

3.0 TiO_2 based photocatalytic systems for pharmaceutical waste treatment

Basic steps involved in the degradation of pharmaceutical pollutants by photocatalysts are shown in Fig. 3. The whole process includes the following: (I) when light from energy higher than the energy band gap of the photocatalyst is absorbed by the photocatalyst, excited electrons and holes with high reducing and oxidizing abilities, respectively, are generated. Thereafter, the photoinduced holes and electrons separate and migrate to the surface of the photocatalyst; (II) some of the electrons and holes recombine to release heat during the migration process; (III) following migration of electrons to the surface of the photocatalyst, a reductive pathway is initiated, wherein O_2 is reduced to $^{\bullet}O_2^-$; (IV) conversely, an oxidative pathway is initiated wherein the holes move to the surface of the photocatalyst, and $^{\bullet}OH$ is generated upon oxidation of H_2O or antibiotic molecules. Then, antibiotic molecules are degraded by the photocatalytic active species $^{\bullet}O_2^-$ or $^{\bullet}OH$. All these processes influence the final rate and efficiency of photocatalytic degradation of antibiotics over the photocatalyst system.[76,115] Therefore, broadening the light absorption spectrum ability of the photocatalysts, enhancing excited charge separation and migration rate, and preventing recombination of the excited charges are expected to effectively improve the activities of photocatalysts.[116] Taking these factors into consideration, there are two key methods of developing highly efficient photocatalysts for photocatalytic degradation of antibiotics: (1) the photocatalyst should have a suitable narrow band gap, which would afford absorption on both UV light and visible light and (2) a suitable separating medium or surface defect state is required, which is capable of trapping photoexcited electrons or holes to prevent their recombination.

3.1 TiO_2 synthesis method

TiO_2 as a photocatalyst is not ideal due to its wide bandgap. Besides, intricate filtration process and distinctly agglomerated opaque solution are crucial restrictions related with nanoparticles for large-scale water purification process.[117] In conjunction, initial adsorption of aqueous phase pollutant on the surface of the photocatalyst is also extremely essential for effective photodegradation reactions to occur.[118] Thus, development of supported photocatalytic systems enables long-term stability, ability to delocalize electrons and sustained oxidative radical attack during irradiation of light.[119] Many techniques, including hydrothermal, sol–gel, and solvothermal methods, have been extensively studied.

3.2 TiO_2 properties: adsorption and photocatalytic activity

3.2.1 Active species. The presence of ions has a huge impact on efficacy of photocatalytic reactions. Ahmed *et al.* (2011)[124] reported that persulfate ions act as electron scavengers and enhance removal efficiency of acridine orange because of the induction of highly reactive $SO_4^{\bullet-}$ (E° = 2.6 eV) radicals, as shown in eqn (1):

$$S_2O_8^{2-} + e_{cb}^- \rightarrow SO_4^{\bullet-} + SO_4^{2-} \quad (1)$$

They suggested three feasible pathways for the production of persulfate with organic molecules: i) eliminating a hydrogen atom from a saturated carbon, ii) reacting with unsaturated or phenolic carbon and, iii) eliminating an electron from carboxylate ions. In conjunction, persulfate may react with the generated electron in the conduction band or with water molecules to induce sulfate ions or hydroxide radicals, respectively, as shown in the equations below:

$$SO_4^{\bullet-} + e_{cb}^- \rightarrow SO_4^{2-} \quad (2)$$

$$SO_4^{2-} + H_2O \rightarrow OH^{\bullet} + SO_4^{2-} + H^+ \quad (3)$$

Eqn (2) shows the improved photocatalytic reaction by reducing electron–hole recombination, whereas eqn (3) shows that produced sulfate ions (SO_4^{2-}) act as an initiator to foster highly reactive hydroxyl radicals. However, at concentrations of persulfate ions beyond the optimum value, the degradation of organic contaminants reduced due to reaction with sulfate ions formed on the TiO_2 surface that contribute to the deactivation of a fraction of catalyst sites. The same trend was observed by (ref. 125) oxidants such as periodate, hydroperoxide, peroxydisulfate and peroxymonosulfate were used in the removal of phenazopyridine. Other ions often found in the water are carbonate ions present in the effluent of water and wastewater sewage. Textile industries use sodium carbonate for fixing dyes on fabric and produce effluents that contain high concentrations of carbonate ions. The carbonate ions function as an inner filter to absorb light energy and radical scavengers and decline the rate of degradation as in the following reactions:[126]

$$CO_3^{2-} + OH^{\bullet} \rightarrow OH^- + CO_3^{\bullet-} \quad (4)$$

$$HCO_3^- + OH^{\bullet} \rightarrow H_2O + CO_3^{\bullet-} \quad (5)$$

The photocatalytic efficiency is considerably decreased when inert salts such as sodium chloride, sodium phosphate, and sodium sulfate or surfactants are present in the water. This is because the adsorption of cationic or anionic molecules occur preferentially on the catalyst surface, while inert salts hinder degradation because of a competitive reaction of ions with holes generated on the photocatalyst surface. For example, for NaCl, the hole scavenging reactions are as shown below, whereby chloride ions, which have a hole

scavenging effect, cause deactivation of holes and inhibit the removal of contaminants (eqn (6)):[126]

$$Cl^- + h^+_{vb} \rightarrow Cl^{\bullet -} + H^+ \quad (6)$$

$$Cl^- + Cl^{\bullet} \rightarrow Cl_2^{\bullet -} \quad (7)$$

Therefore, the existence of organic or some inorganic species such as chloride ions can impact the degradation rate and effectiveness of the process (since part of $^{\bullet}OH$ is used by these species); therefore, a total mineralization of wastewater is required. This is because a complex medium contains hundreds of species, thus influencing the photocatalytic process efficacy.

3.3 Limitation of TiO_2 in photocatalytic systems

In recent years, by use of antibiotics contamination due to a wide range of human activities has gained special attention. Thus, development of solar light driven photocatalysis as a "green technology" for wastewater treatment has been studied. For almost 40 years, by Fujishima and Honda, have been continuously exploring photocatalytic activity of TiO_2 (ref. 9) as a promising approachable technology for water treatment processes that could significantly enable reduction of pharmaceutical pollution based by harnessing light energy.[33,34,36–40] In addition, under visible light irradiation, the effectiveness of TiO_2 to self-induce highly active scavengers such as hydroxyl radicals provide favorable properties (*e.g.*, non-toxicity, no dissolution in water, photostability), making TiO_2 a suitable candidate for the complete mineralization of emerging pollutants[41,42] in photocatalysis.

However, some disadvantages of TiO_2 include fast recombination between electron–hole pairs, efficient activation with the only UVC due to a band gap energy of 3–3.2 eV, difficult recovery of TiO_2 nanoparticles from treated liquid, and agglomeration, which are detrimental to its use in photocatalysis.[127] Besides, with its wide band gap (3.2 eV), only 5% of UV light can be pass through, thus hindering its applications in large-scale wastewater treatment. Therefore, introducing semiconductor photocatalysts such as Ag_3PO_4, CdS, Cu_2O, ZnS, and PbS helps narrow the band gap, thus increasing visible light activity.[45,46] However, light-driven photocatalyst can not be used as an efficient photocatalyst in waste water treatment. Therefore, difficulties in separation of photocatalyst from treated water, especially from a large volume of water, is a troublesome process. Moreover, sedimentation and centrifugation processes are demanding at industrial scale because of long time duration and technical limitations.[39] Besides, Pastrana-MartAnez *et al.* have stated that use of TiO_2 photocatalyst involves two drawbacks: (1) low quantum yield predominantly impeded by recombination of electrons and holes and (2) unsatisfactory ability to harness light limited by the wide band gap of TiO_2 to absorb the UVA spectral range.[29] Other limitations are TiO_2 powders are prone to deposit after a while resulting in a decline of amount of light absorbed and in lower effectiveness and efficiency.

This design for more efficiency of TiO_2 *via* various methods such as ion doping, incorporation of semiconductor compound, dye photocatalyst, noble metal deposition, *etc.* was fabricated. A highly attractive alternative toward the development of photocatalysts based on nanoscale composites depends on the association of TiO_2 with carbon materials such as mesoporous carbon, carbon nanotubes[44–46] or more recently graphene-based TiO_2.[32]

4.0 TiO_2 hybrid photocatalytic systems for pharmaceutical waste treatment

Recently, heterojunction photocatalytic systems or hybrid photocatalytic systems, which constitute a combination of two semiconductors with matching energy band gaps, have attracted much attention because they are effective alternatives to separate photo-induced charges, thereby improving photocatalytic performance.[128] Heterojunction architectures are classified into three main groups denoted as type I, type II, and type III.[69] Of the three photocatalyst systems, type II heterojunction is believed to show the most potential in realizing the highest photocatalytic efficiency as the configuration can effectually impede recombination of electrons and holes. The typical mechanism for photo-generated charge transfer in type II heterojunction photocatalyst systems is illustrated in Fig. 4. As observed, the photoexcited electrons can migrate from semiconductor I to semiconductor II in a type II heterojunction owing to the more negative conduction band position of semiconductor I. Simultaneously, because of the more positive valence band of semiconductor II, photoexcited holes can migrate in the opposite direction to that of electrons, leading to complete effective charge separation.[51] Furthermore, type II heterojunction is conducive to regulating the range of light absorption. To date, development of type II heterojunction photocatalyst systems and many advanced heterojunction photocatalysts with enhanced photocatalytic antibiotic degradation efficiency under visible-light irradiation has been widely studied (Fig. 2).[70]

Much effort has been directed to designing and fabricating visible-light-driven photocatalysts, and diverse advanced photocatalytic materials have been designed for the treatment of antibiotic wastewater.[50,51] Four main strategies have been employed: (1) doping of UV light-driven photocatalysts with metals and non-metals; (2) development of new visible-light-driven semiconductor photocatalysts; (3) design and construction of heterojunction photocatalysts with nanocarbons; and (4) design and construction of surface plasmon resonance (SPR)-enhanced photocatalytic systems.

4.1 Magnetic photocatalytic system of TiO_2/metal oxide for pharmaceutical waste treatment

4.1.1 TiO_2/Fe_3O_4 hybrid photocatalytic system. Photocatalysis with TiO_2 has been studied with propitious results

in mineralizing a series of pharmaceutical pollutants. Designing of magnetic TiO_2/Fe_3O_4 and $TiO_2/SiO_2/Fe_3O_4$ nanoparticles (NPs) by a simple sol–gel technique assisted with ultrasonication for removal and mineralization (*i.e.*, TOC removal) of five selected pharmaceutical pollutants from aqueous solution was reported.[40] In this study, a method to improve the separation of TiO_2 is evaluated through the fabrication of nanoparticles (NPs) and a magnetic core (Fe_3O_4) with a TiO_2 shell. This is conducted to ease separation of pollutants from the treated water under exposure of external magnetic waves. Beydoun and co-workers modeling for magnetically separable photocatalysts is a pioneer in this field. Most TiO_2 photocatalyst-based magnetic fields investigated to date contain ferum element such as magnetite (Fe_3O_4), maghemite (γ-Fe_2O_3) or ferrite (*e.g.*, $NiFe_2O_4$).[6,7,29–31] Introduction of a barrier layer of SiO_2 wafer between the magnetic core and TiO_2 shell has been suggested to prevent photo-dissolution of ferum as well to hamper recombination of electrons and holes that decreases the photocatalyst activity.[7,31–33] TiO_2 photocatalysis based magnetic properties have already been identified for the degradation of pharmaceutical pollutants, dyes and phenol in most cases.[34,36–38] Predominantly, favorable results of photocatalytic activity, separability, and catalyst stability have been noted.

Besides, another study has investigated spinel ferrites TFe_2O_4 (M = Mn, Co, Zn, Ni, Mg, *etc.*), as they are well-known for their cubic spinel characteristic, whereby oxygen atom forms a face-centered cubic (fcc) close packing and T^{2+} and Fe^{3+} are filled either in the interstitial sites of tetrahedral or octahedral sites.[6,7] Thus, considering the highly stable crystal structure along with an excellent magnetic field and chemical stability of spinel ferrites, extensive uses in application such as optoelectronics, drug-loading materials, spintronic devices, and microwave adsorption have been implied. Manganese ferrite ($MnFe_2O_4$) with promising magnetism and functional surface has been vastly used in water purification technology.[31] This is because $MnFe_2O_4$ has good adsorption capacity and biocompatibility and higher magnetism than $NiFe_2O_4$, $CoFe_2O_4$, and $CuFe_2O_4$ nanoparticles.[58] Lin *et al.* have studied the photocatalytic oxidation of pharmaceuticals waste by TiO_2–Fe nanocomposites by measuring degradation of three pharmaceuticals (ibuprofen, carbamazepine and sulfamethoxazole) under UV and visible light irradiation. The results suggest that the enhanced photocatalytic performance

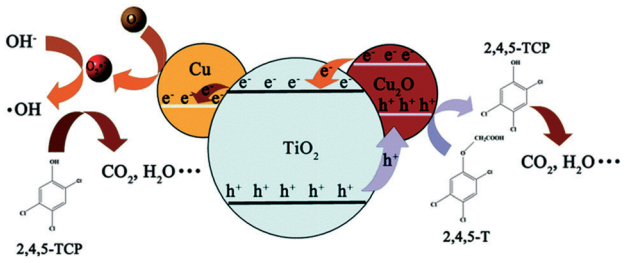

Fig. 2 Schematic of the mechanism of photo-generated charge transfer in a (type II) heterojunction photocatalyst system.[69]

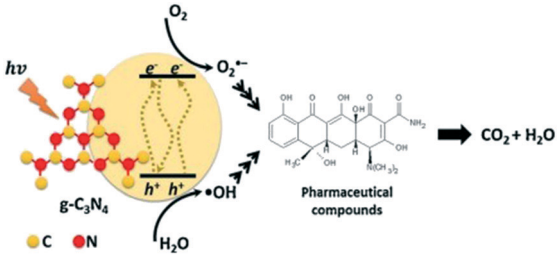

Fig. 3 Narrow band gap of graphene carbon nitride allows efficacious light absorptivity within UV-visible light range for effective photocatalytic degradation of pollutants.[151]

of TiO_2–Fe nanocomposites could be attributed to their narrower band gap.[129] High photoactivity of TiO_2–Fe can be also ascribed to new impure levels introduced between the conduction and valence band of TiO_2, from which the electrons can be excited to the conduction band. Therefore, TiO_2–Fe has a narrower band gap (2.40 eV) than pure TiO_2 (3.20 eV), resulting in increased absorption in the visible-light region.[130] However, small size, agglomeration of nanosized ferrites and magnetic interaction make recuperation of photocatalyst during large-scale water purification process[37] complicated. Thus, a highly efficacious degradation reaction by visible light occurring on the photocatalyst surface[18] is a pre-requisite to develop supported photocatalytic systems involving immobilization of nanosized metal oxide particles onto appropriate support materials. The support materials should have high stability, long half-life and ability to withstand radical attack during exposure to light.[39]

4.1.2 TiO_2/CuO hybrid photocatalytic system. It is reported that heterogeneous photocatalytic oxidation technologies are propitious techniques and a number of papers on photocatalytic advanced oxidation technologies are aimed at dye/TiO_2 system.[29] Several ways to enhance the performance of catalysts, for instance, doping the catalyst to narrow the band gap,[31,32] structuring the catalyst in nano-size[34] and combining a narrow-bandgap and wide-bandgap semiconductor[39–41] have been reported. A recent study shows that Cu_2O can catalyze the emerging pollutants of water into H_2 and O_2 under visible light due to excellent catalytic performance and stability of Cu_2O.[41] In addition, nanosized Cu_2O photocatalyst displays an excellent elimination of dye pollutants with a high

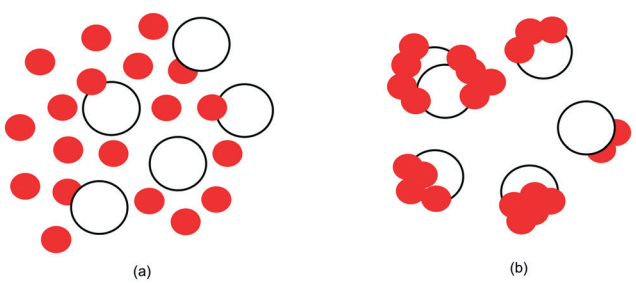

Fig. 4 (a) Higher pH leads to more availability of hydroxyl ions on the TiO_2 surface, whereas (b) lower pH of the solution in photochemical reaction promotes aggregation.

degree of mineralization[42] when exposed to visible light. In this regard, when a heterostructure forms between TiO_2 and Cu_2O, it can aid in promoting the dissociation and movement of photo-generated charge carriers in TiO_2/Cu_2O composite, thus reducing the possibility of recombination and in turn promoting photocatalytic properties.

Yi *et al.*,[131] synthesized nanoscale TiO_2/Cu_2O heterostructure composite through an alcohol aqueous-based chemical precipitation method. Photocatalytic activities of the nanocomposite catalysts were explored in terms of decomposition action on methyl orange dye. Results revealed that the formation of a hetero-interface between Cu_2O and TiO_2 aids the dissociation and movement of photoinduced charge molecules and impairs the possibility of recombination, thus leading to with greatly increased photocatalytic activity. The effect of adding 5–12.5 wt% CuO to TiO_2 on photocatalytic properties of the nano-composite TiO_2/CuO was investigated by Koohestani *et al.*[132] BET specific surface area of the TiO_2/CuO composites was lower than that of pure TiO_2. Incorporation of CuO into TiO_2 shifted absorption spectra to the visible region. As CuO content increased from 0 to 12.5%, a clear decrease in optical band gap from 2.95 to 2.30 eV was observed. The photocatalytic performance was determined under ultraviolet irradiation. However, the excessive incorporation of CuO did not improve the ability of TiO_2 to degrade MeO and cyanide. The highest rate of photocatalytic degradation was found in TiO_2–7.5% CuO. The rate constants of degradation reaction using TiO_2 and TiO_2–7.5% CuO catalysts were 0.0107 and 0.0151 min^{-1}, respectively. Another study on a dual Z-scheme TiO_2–Ag–Cu_2O photocatalytic system was also conducted, wherein Cu_2O was loaded onto electrospun TiO_2 nanotubes by an easy impregnation–calcination process, and Ag was subsequently deposited onto the photocatalyst through a photo-deposition method. Under UV-vis light irradiation, both TiO_2 and Cu_2O can be excited. The photoinduced electrons from the conduction band of TiO_2 excited to Ag due to formation of a lattice vacancy on the metal–semiconductor matrix, while SPR-induced local electric field drove the electrons of Ag to recombine with holes of Cu_2O on the valence band. Lastly, electrons in the conduction band of Cu_2O reacted with H^+ to generate hydrogen gas, resulting in a greatly improved photocatalytic performance for hydrogen generation.

4.2 Magnetic photocatalytic system of TiO_2/metal hybrid for pharmaceutical waste treatment

Development of a photocatalyst driven by visible light that harnesses the utilization of effective solar energy[46] has been a focus by many researchers. Incorporation of metals ions is a propitious technique as it helps in the dissociation of electron–hole pairs and improves light absorption capability.[7] Besides, their distinct properties such as structural pliability and large surface area to volume ratio have led to the successful development of metal–organic frameworks (MOFs) in adsorption, sensor devices, catalysis, magnetism and drug release. Thus, to retain photocatalytic performance of MOFs, studies on the introduction of functional elements into such materials in fabricating metal-MOF nanocomposites have been conducted.[47,48]

4.2.1 TiO_2/Ag hybrid photocatalytic system. To date, noble metal–TiO_2 composites have been applied vastly in the field of photocatalysis.[37,38] When the nanoparticles of a noble metal, such as Au, and a catalyst, TiO_2, are bound to form the composition the charge will allocate. From the Fermi levels, nanoparticle noble metals (Au, Ag, or Pt) are lower as compared to TiO_2, resulting in the excitation of photoinduced electrons from the conduction band of TiO_2 towards the surface deposited noble metal.[39] Moreover, when the size of metal is reduced, it displays excellence light absorption in the visible light are due to collective oscillation of valence electrons of the metal.[40] Therefore, coupling nanoparticle noble metal adjoin with TiO_2 can inhibit recombination of photoinduced electrons and holes and widen the absorption rate of light in the visible light region, thus improving photocatalytic activity.[41]

Yi and group investigated Ag_3PO_4 and TiO_2 and stated that it possessed excellent photoreaction catalyst activity for the deterioration of organic emerging pollutants and water splitting.[131] Even though Ag_3PO_4 showed good application in photocatalyst driven reactions, pure Ag_3PO_4 always shows poor stability due to the photo-corrosion and precipitation. However, fashion the composite of Ag_3PO_4 to ameliorate the defects has been a keen interest among researchers. For example, the modeling and fabrication of a unique assembled heterostructure, can be combined with other semiconductors, by loading onto supports, doping ions, and so forth. Wang *et al.*[137] studied reaction conditions (temperature and time) and observed that the morphology of Ag_3PO_4 depends on photocatalyst activity and methylene blue was affected by the morphology. This was predominantly owing to the distinct framework and improved adsorption of surface morphology as well as enhanced dissociation between electrons and holes. On the other hand, Bi *et al.*[134] reported that by regulating various facets of single crystalline Ag_3PO_4 could efficaciously improve photoreaction of catalyst on methyl orange and Rhodamine B. Also, Zhang *et al.*[127] noted that Ag_3PO_4 doped Bi^{3+} ions can tremendously influence electronic composition and diminish surface hydroxyl group defect, simultaneously affecting the behavior of Ag_3PO_4 particles. Ternary TiO_2–SiO_2–Ag nanocomposites with enhanced visible-light photocatalytic activity were synthesized by Liu *et al.* through a facile biomimetic approach by utilizing lysozyme as both an inducing agent of TiO_2 and reducing agent of Ag^+.[135] TiO_2 nanoparticles (~280 nm) were first fabricated by inducing lysozyme. Afterward, SiO_2 layers were formed as "pancakes" stuck out of TiO_2 nanoparticles through a sol–gel process. Finally, Ag nanocrystals (~24.5 nm) were deposited onto the surface of TiO_2–SiO_2 composites *via* reduction of lysozyme, forming TiO_2–SiO_2–Ag nanocomposites. The resultant nanocomposites displayed a high photocatalytic activity under visible-light irradiation, which can be attributed to the synergistic effect

of enhanced photon absorption because of surface plasmon resonance of Ag nanocrystals and the elevated adsorption capacity of Rhodamine B because of the high specific surface area of SiO_2. This study may provide some inspiration for the rational design and facile synthesis of composite catalysts with high and tunable catalytic property through a green, efficient pathway.

4.2.2 TiO_2/CdS hybrid photocatalytic system. In the study reported by Park *et al.*,[70] CdS incorporated graphene/TiO_2 composite was synthesized by a comparative sol–gel process and precipitation reaction, wherein $Cd(NO_3)_2$ solutions and the $Cd(NO_3)_2$ and Na_2S solutions and titanium oxysulfate were used. Improved TiO_2 and CdS-incorporated graphene was investigated as a new photocatalytic CdS-graphene/TiO_2 nanocomposite. Their structural attributes were characterized by XRD, SEM, TEM, and EDS. Methylene blue was selected as a typical dye to examine the photocatalytic properties of CdS incorporated graphene/TiO_2 under UV light. The degradation mechanism and kinetics of the catalysts driven by visible light were also studied. In addition, Li *et al.* successfully designed a TiO_2/Au/CdS heterojunction Z-scheme photoanode and discovered that its electrochemical-based visible-light performance was better than that of TiO_2/CdS material.[71] One-dimensional (1D) CdS@TiO_2 core–shell nanocomposites (CSNs) were successfully synthesized *via* a two-step solvothermal method by Liu *et al.*[136] The results demonstrated that a 1D core–shell structure is formed by coating TiO_2 onto the substrate of CdS nanowires (NWs). The visible-light-driven photocatalytic activities of the as-prepared 1D CdS@TiO_2 CSNs were evaluated by selective oxidation of alcohols to aldehydes under mild conditions. Compared to bare CdS NWs, an obvious enhancement of both conversion and yield was achieved in 1D CdS@TiO_2 CSNs, which is ascribed to the prolonged lifetime of photogenerated charge carriers in 1D CdS@TiO_2 CSNs under visible-light irradiation. Furthermore, it was shown that the photogenerated holes from CdS core can be stuck by the TiO_2 shell, as evidenced by controlled radical scavenger experiments and efficient selective reduction of heavy-metal ions, Cr(VI), over 1D CdS@TiO_2 CSNs; consequently, it was found that the reaction mechanism of photocatalytic oxidation of alcohols over 1D CdS@TiO_2 CSNs is apparently different from that over 1D CdS NWs under visible-light irradiation. It is hoped that our work could not only offer useful information on the fabrication of various specific 1D core–shell nanostructures but also open a new doorway for such 1D core–shell semiconductors as visible-light photocatalysts in the promising field of selective transformations.

4.2.3 TiO_2/Cu hybrid photocatalytic system. The potential of TiO_2 as a catalyst in photocatalytic is enhanced by improving UV light harvesting and hindering recombination of electrons and holes by mixing with a semiconductor, assembly with a noble metal, and hydrogenation or doping of a transition metal.[6,7] Among the different techniques, devising TiO_2 heterojunctions using semiconductors with more negative and narrow conduction band edge positions is a practical method to improve photocatalytic activity of TiO_2. TiO_2/semiconductor heterojunction not only raises the potential gradient at the interface to boost dissociation of electrons and holes by excitation of electrons from an excited-state-bandgap semiconductor into a ground-state bandgap semiconductor,[31] but also aids in a wide range of visible light absorption. Copper sulfide, an n-type semiconductor material with a narrow band gap of 2.0 eV, also displays outstanding characteristic in photocatalysis. Assembling CuS–TiO_2 composite enhances adsorption of visible light on surface morphology while enhanced the limiting electrons and holes separation. For example, Li *et al.*[70] have designed a unique micro/nano-scaled TiO_2/CuS composition incorporated fibers using an electrospinning method. The micro/nanocomposite fibers displayed a robust visible-light performance and excellent efficiency of electron–hole separation compared with unalloyed TiO_2 fiber. Ratanatawanate *et al.*[32] have investigated TiO_2 nanotubes with CuS quantum dots through a series of CuS nanoparticle crystallizations and have shown that photocatalytic performance and photosensitivity of TiO_2 nanotubes in the visible light region are improved by the presence of CuS quantum dots. Im *et al.*[36] have designed a shell-structured CuS/TiO_2 photocatalyst, which have a potential to absorb a wide wavelength of above 700 nm. The electrons from the valence band of CuS are excited by the existence of TiO_2, leading to a faster rate of electron–hole pair dissociation and higher photocatalytic performance.

4.3 Highly selective photocatalytic system for pharmaceutical waste treatment

4.3.1 TiO_2: nano-carbon hybrid photocatalytic. The commercial use of TiO_2 is demanding because of the costly treatment in dissociating treated sewage from active persistent light micromolecules. Thus, a technique for solving this issue is the utilization of supports,[118] which give auxiliary benefits, such as enhanced chemical and thermal stability, as well as an improved surface area for the catalytic material, which results in higher performance.[119] Thus, numerous studies have been conducted on various kind of supports, such as clay, graphene, zeolites and activated carbon owing to their fast charge transfer, efficient charge separation, superior specific surface area and electrical conductivity. Assembling of visible-light-driven photocatalytic systems using graphene materials can effectively increase the migration of photogenerated electrons and holes and enhance photoinduced charge separation to achieve high photocatalytic efficiency. Wang *et al.* reported the synthesis of hybrid TiO_2:carbon hollow spheres by a facile and green method using a carbon nanosphere template.[130,137,138] In this work, the carbon content of the TiO_2:carbon hybrid was adjusted by changing the duration of the final calcination step, which was shown to significantly affect physicochemical properties and photocatalytic activity of the hybrid.[139,140] The optimized TiO_2:carbon hybrid exhibited enhanced photocatalytic activity

compared with commercial TiO_2 (P25).[141,142] The significantly improved photocatalytic activity was not only due to the increased specific surface area, but also due to a local photothermal effect around the photocatalyst caused by carbon.[143] The preparation and photocatalytic properties of hybrid nanofibers/mats of anatase TiO_2 nanoparticles and multi-walled carbon nanotubes (MWNTs) using combined sol–gel and electrospinning techniques was reported by Hu *et al.*[144] Poly(vinyl pyrrolidone) was used as a base polymer in the electrospinning suspension to assist the formation of nanofibers and was subsequently removed by calcination. The hybrid nanofibers were characterized using XRD, Raman spectra, FT-IR, XPS, SEM, TEM and N_2 adsorption measurements. The results showed that MWNTs were encapsulated by *in situ* formed anatase TiO_2 nanoparticles, with chemical bonding C–O–Ti between anatase TiO_2 nanoparticles and MWNTs. Hybrid nanofibrous mats with moderate content of MWNTs (mass ratio TiO_2 : MWNTs = 100 : 20) exhibited enhanced adsorption ability and excellent photocatalytic activity. The composition, diameter, and morphology of hybrid nanofibers could be tuned by varying sol–gel formulation, electrospinning parameters and post-treatment conditions. TiO_2/MWNTs hybrid nanofibers and mats have promising applications in water purification.

4.3.2 TiO_2/CNTs hybrid photocatalytic system. The introduction of metals and nonmetal materials like multi-wall carbon nanotubes (MWCNTs) in TiO_2 has been studied to overcome this limitation.[145] Previous studies show that the performance of photocatalytic TiO_2 can be enhanced by forming composites assembled with MWCNTs.[89] MWCNTs function as a bed to prepare transition metal supported catalysts and allocate dispersions of functional materials to improve their functionalities including high metallic conductivity, large electron-storage capacity, wide light range absorption and large surface area to volume ratio.[126] MWCNTs enable trapping of electrons, transferring them from TiO_2, and stabilize charge separation, thus impeding electron–pair recombination. This can be elucidated which MWCNTs is acting as a stimulator and boosting the injection of photoexcited electrons from TiO_2 to reduced recombination of holes and electrons.[117,121] Moreover, MWCNTs serve as a dispersing bed for reducing agglomeration of TiO_2 nanoparticles.[125] A carbon nanotube (CNT)/TiO_2 photocatalyst nanocomposite has been prepared by a simple impregnation method, which is used, for the first time, for gas-phase degradation of benzene. It is found that the as-prepared CNT/TiO_2 nanocomposite exhibits an enhanced photocatalytic activity for benzene degradation, as compared with commercial titania (Degussa P25). A similar phenomenon has also been found for liquid-phase degradation of methyl orange. CNT has two kinds of crucial roles in the enhancement of photocatalytic activity of TiO_2. One is to act as an electron reservoir, which helps to trap electrons emitted from TiO_2 particles due to irradiation by UV light, thus hindering electron–hole pair recombination. The other is to act as a dispersing template or support to control the morphology of TiO_2 particles in the CNT/TiO_2 nanocomposite.[141] Based on literature review, there is no report about photocatalytic degradation of TC using MWCNT/TiO_2 nano-composite; however, in some studies, MWCNT/TiO_2 nanocomposite has been fabricated to improve the performance of photocatalyst TiO_2 nanoparticles for photo-decomposition of pharmaceutical pollutants in the aqueous phase and in wastewater. The effect of operational parameters including ration of MWCNT to TiO_2 ratio, photocatalyst dosage, pH, concentration and irradiation time have been identified, and subsequently, a real pharmaceutical wastewater sample undergoes photocatalytic treatment.

4.3.3 TiO_2/activated carbon hybrid photocatalytic system. Many researchers have explored the immobilization of TiO_2 nanoparticles on various support materials to enhance visible-light-driven photocatalytic performance and enable more effective dissociation of treated sewage.[53] Activated carbon (AC), a unique carbon material, displays large specific surface area to volume ratio, low cost and high adsorption performance, which enhances photocatalytic reaction between TiO_2 catalyst and pollutant.[59] AC has vastly been used as an adsorbent for active hydrocarbons pollutants.[54] Thus, investigation of photocatalyst Ag–Ag_3PO_4 incorporating AC has been investigated using a facile deposition and photo-generated technique, and the photocatalytic activity is evaluated by decomposition of tetracycline.[125] The loaded Ag_3PO_4 photocatalysts exceptionally aids in photocatalytic activity and characteristics of Ag/Ag_3PO_4 incorporated AC composites such as crystalline structure, photocatalytic activity, and optical properties.

Another investigation of solar photocatalytic oxidation using TiO_2 *versus* TiO_2/AC to study its efficiency for degradation of pharmaceuticals was reported.[146] Amoxicillin, ampicillin and two other prevalent drugs (diclofenac and paracetamol) were used as model substrates. Characterization was carried out and factors affecting photodecomposition such as a change in pH and amount of TiO_2/AC catalyst loading were studied. Besides, the first order kinetics was evaluated according to the Langmuir–Hinshelwood model. Conclusively, the supports play an important role in photocatalytic performance and stability.

A sequential adsorption/photocatalytic regeneration process to remove tartrazine was investigated.[147] The aim of this work was to compare the effectiveness of an adsorbent/photocatalyst composite – TiO_2 deposited on activated carbon (AC) – and a simple mixture of powders of TiO_2 and AC in the same proportion. The composite was an innovative material as TiO_2, was deposited on the porous surface of a microporous AC using metal–organic chemical vapor deposition on a fluidized bed. The sequential process comprised two-step batch cycles: every cycle alternated a step of adsorption and a step of photocatalytic oxidation under ultra-violet (365 nm) light at 25 °C and atmospheric pressure. Both steps, adsorption and photocatalytic oxidation, were investigated during four cycles. For both materials, the cumulative amounts adsorbed during four cycles corresponded to nearly twice the

maximum adsorption capacity q_{max}, proving the photocatalytic oxidation and adsorption. Concerning photocatalytic oxidation, the degree of mineralization was higher with the TiO_2/AC composite: for each cycle, the value of total organic carbon removal was 25% higher than that obtained for the mixture powder. Better photocatalytic performances involved better regeneration and higher adsorbed amounts for cycles 2, 3 and 4. Better performance with this promising composite compared with TiO_2 powder can be explained by the vicinity of photocatalytic and AC adsorption sites.

4.3.4 TiO_2/graphene hybrid photocatalytic system. Graphene, a 2D nanostructure, renders exciting opportunities for future-generation photocatalysts as graphene oxide can be easily obtained by scaling of graphite oxide,[47] contributing a 2D substrate equipped by oxygen atoms at the bases and edges of planes, providing abundant active and attached sites for construction of graphene-based nanocomposites.[49] Besides, graphene oxide is governed by the interaction of excited π-states from sp2 carbon atoms to sp3 matrix within a large energy bandgap (σ-states), showing an extremely heterogeneous electronic composition.[50] This, in turn, may thoroughly alter graphene oxide electronic properties from the "conductor-like" up to the graphene-like semi-metallic state under favorable processing conditions. Hence, notable improvement in visible-light-driven photocatalytic performance has been gained when graphene oxide combined with TiO_2, due to their intersurface electron transfer and significantly improve adsorption ability.[32]

Kamat and co-workers[51,52] have reported that electrons induced on TiO_2 upon UV light irradiation are excited and eventually transfer across to the graphene oxide layer, causing recombination between electrons and holes on the composite under UV irradiation. Considerable research has led to extensive investigation on fabrication of efficacious graphene oxide/TiO_2 photocatalyst composites utilizing various synthetic pathways that potentially harness graphene oxide as an excellent adsorptive material acting as a scavenger and transport system for electrons, thus improving light-driven photocatalytic activity.[35,148] Previous study focused on constructing solid material-activity interaction by using the reduced graphene oxide/TiO_2 photocatalyst composites, as well as investigating their ability as an effective visible-light-driven photocatalyst. It was found that emerging pollutants found in sewage and industrial wastewater have a low tendency to be decomposed by microorganisms;[149] however, their distinct absorption properties aids in offering feasible improvement in photocatalytic performance. The prominent quenching of graphene oxide photoluminescence under UV laser excitation and improved radical mediated oxidation manifested by scavenger trapping experiments showed that reduced graphene oxide can serve as a light sensitizer of TiO_2. Therefore, it is proposed that reduced graphene oxide/TiO_2 heterostructures allow TiO_2 photocatalysis in the UV light range without weakening its performance upon irradiation.[150]

To date, graphitic carbon nitride has been recognized among researchers due to its narrow band gap, leading to the efficacious light absorptivity within the UV light range, which is as illustrated in Fig. 3.

This distinct characteristic and its electrical conductivity make it favorable for future applications and theories.[152] Wang *et al.* have successfully synthesized hydrogen using graphitic carbon nitride as a photocatalyst.[156] Since then, H_2 evolution and organic degradation has been vastly explored. Nonetheless, pure graphitic carbon nitride has some shortcomings, such as easy recombination of photoinduced electrons and holes, prompting low performance.[154] Nanocomposites of TiO_2–graphene (TiO_2–GR) have been prepared *via* a facile hydrothermal reaction of graphene oxide and TiO_2 in an ethanol–water solvent.[155] We show that such a TiO_2–GR nanocomposite exhibits much higher photocatalytic activity and stability than bare TiO_2 toward gas-phase degradation of benzene, a volatile aromatic pollutant in air. By investigating the effect of different addition ratios of graphene on the photocatalytic activity of TiO_2–GR systematically, we find that the higher weight ratio of TiO_2–GR decreases photocatalytic activity. An analogous phenomenon is also observed for liquid-phase degradation of dyes over TiO_2–GR. In addition, the key features for TiO_2–GR including enhancement of adsorptivity of pollutants, light absorption intensity, electron–hole pair lifetime, and extended light absorption range have also been found in the composite of TiO_2 and carbon nanotubes (TiO_2–CNT). These strongly show that TiO_2–GR is, in essence, the same as other TiO_2–carbon (carbon nanotubes, fullerenes, and activated carbon) composite materials with respect to enhancement in photocatalytic activity of TiO_2, although graphene by itself has unique structural and electronic properties. Therefore, various graphitic carbon nitride photocatalysts have been fabricated to enhance optimum absorptivity of visible light. In another investigation, preparation of various graphene oxide–TiO_2 composites liquid phase precipitation method using ammonium hexafluorotitanate as TiO_2 starting material has been reported. Results show an optimum GO content yield of 3.3–4.0 wt% at 200 °C. This favorable environment in yielding composites is higher in photocatalytic activity than P25 in the decomposition of methyl orange (MO) dye and diphenhydramine (DP) pharmaceutical upon illumination in near UV and visible region.

4.3.5 TiO_2/nano cellulose fiber hybrid photocatalytic system. In spite of the long lifespan and dependability of TiO_2 catalyst, the dissociation and recuperation processes have proved to be major challenges in application in sewage treatment processes. Recent studies have reported that nano-sized metal oxide materials could trigger unfavorable effects in aquatic environments, suggesting post-processing is required after using TiO_2.[66,67] Therefore, to resolve these setbacks, implementation of nanofiber (NF)-photocatalyst is more beneficial as it improves catalytic performance and provides a large surface area per unit volume ration[90] and easy water splitting. This is predominantly attributed to its distinct morphology along with nanotube groups.[55] Modeling of TiO_2 NFs by

electro-spinning was first reported in 2003.[45] Since then, various types of TiO_2 NFs have been synthesized, for instance, polypyrrole-Ag–TiO_2 NFs, nano-CdS complex sensitized electrospun TiO_2 NFs, and iron phthalocyanine-TiO_2 NF heterostructures; hollow mesoporous TiO_2 NFs show a better photocatalytic performance than TiO_2 NPs and Au co-catalyzed TiO_2 NFs.[121]

Shen and co-workers (2014)[45] synthesized TiO_2 nanofibres (NFs) by electrospinning. They electro-spun the starting material of the solution, followed by hot pressing to improve the adhesion of TiO_2 NF films to a conductive support for facilitating the use of photocatalysts more than once without supplementary dissociation. Preparation of an optimum photocatalytic environment was determined by investigating the oxidation rate of furfuryl alcohol (FFA) under ultra-violet illumination. In addition, the influence of pH on decomposition of three pharmaceuticals pollutants, carbamazepine, cimetidine, and propranolol, was investigated using deactivated substrate TiO_2 NFs. Another report investigated TiO_2 nanofibers (NFs) on the surface of a stainless steel filter with the aid of a binder layer, poly(vinylidene fluoride) (PVDF). PVDF enables adhesion of photocatalyst nanoparticles on to the stainless steel filter for designing a multi-purpose visible-light-driven photocatalyst. By doing so, diffusion restriction of contaminants to the surface of photocatalysts was minimized. Thus, deactivation performance of photocatalyst can be significantly refined, and resilient deactivation of TiO_2 nanoparticles can effectively reduce possible hazardous outcomes on human health and environment.[25] Herein, decomposition of pharmaceutical compounds such as acetaminophen, sulfamethoxazole, and propranolol was noted.

Studies on photocatalytic activity of TiO_2 incorporated coconut shell powder (TCNSP) nanocomposite for photodegradation of three PPCP pollutants under UVC (254 nm) and black light blue UVA (365 nm) irradiation have been conducted. The physicochemical properties of the prepared TiO_2–coconut shell powder (TCNSP) composite have been fully characterized and reported previously.[44] Studies shows that photocatalytic reaction rate of PPCPs decreased with inclining initial concentration of PPCPs, but increased with increasing TCNSP concentration, light intensity and dissolved oxygen concentration. The removal trends were UVC/TCNSP > UVA/TCNSP > UVC > UVA. The pH has a major influence on the UV/TCNSP composite process, whereby TCNSP composite and commercial GAC showed 99% and 90% removal efficiency, respectively. Conclusively, TCNSP composites were reused and after five runs, 80% of carbamazepine removal still maintained, whereas removal efficiency of other adsorbents decreases dramatically with remarkable deactivation.

4.4 Reaction mechanism pathway studies on TiO_2 based photocatalytic systems for pharmaceutical waste treatment

The stages involved in photocatalytic degradation are illustrated in Fig. 3. The entire process includes the following: (I) when light from energy higher than the band gap of the photocatalyst is absorbed by the photocatalyst, excited electrons and holes, with high reducing and oxidizing abilities, respectively, are generated. Thereafter, the photoinduced holes and electrons separate and migrate to the photocatalyst surface; (II) some of the electrons and holes recombine to liberate heat during the migration process; (III) following migration of the electrons to the surface of the photocatalyst, a reductive pathway is initiated, wherein O_2 is reduced to $^{\bullet}O_2^-$; (IV) conversely, an oxidative pathway is initiated when the holes migrate to the surface of the photocatalyst and $^{\bullet}OH$ is generated upon oxidation of H_2O or the antibiotic molecules. Then, toxic molecules (TMs) are degraded by active photocatalytic active $^{\bullet}O_2^-$ or $^{\bullet}OH$. All these processes influence the final rate and efficiency of photocatalytic degradation of TM over the photocatalyst system.[27,28] Therefore, broadening the light absorption spectrum ability of the photocatalysts, enhancing excited charge separation and migration rate, and preventing recombination of the excited charges are expected to effectively improve photocatalytic activity.[49] Taking these factors into consideration, there are two key methods for developing highly efficient photocatalysts for the photocatalytic degradation of antibiotics: (1) the photocatalyst should have a suitable narrow band gap, which would yield absorption of both UV light and visible light respectively and (2) a suitable separating medium or surface defect state is required, which is capable of trapping the photoexcited electrons or holes to prevent their recombination.

4.4.1 Effect of the amount of catalyst in photocatalytic systems on pharmaceutical waste treatment. Reduction loading of catalyst reduces the number of absorbed photons absorbed and decreases the degradation rates.[89] Reducing the amount of catalyst increases solution transparency, which increases penetration of photon flux in the reactor and thus declines photocatalytic decomposition performance.[73] Other studies reported that "the loading of catalyst brings both pros and cons on the photodegradation activity." Their studies revealed the initial reaction rates were directly related to the catalyst loading in heterogeneous pattern. Various amounts of Degussa P25 were studied in the range of 0.5–5 g l^{-1} to observe decomposition kinetics of gentian violet. Results showed the decomposition performance of the dye was found to increase with amount of catalyst.[115,116] Besides, Qamar and co-workers (2005)[120] discovered that the decomposition rate of chromotrope 2B and amido black 10B increased with addition of loading catalyst in various concentrations (varying from 0.5 to 5 g l^{-1}) of Degussa P25. Another investigation by Zhou and Wang,[156] in agreement with Saggioro group, found that the decomposition rate of Orange G is *pro rata* to TiO_2 loading (from 300 to 2000 mg l^{-1}). Zhang *et al.* (2002)[153] evaluated the reliability of photocatalytic kinetics of methylene blue on the amount of loaded TiO_2 and noted the rates inclined with the addition of TiO_2 until a threshold level and then decreased to a constant value. Aniline is one of the most toxic pollutants and it is released into the environment after its use in manufacturing pharmaceuticals. The effect of photocatalyst (TiO_2)

concentration on the degradation of aniline was investigated by Mansouri *et al.* The experiments were conducted using various amounts of TiO_2. The effects of the amount of TiO_2 on removal of aniline were significant, confirming the positive influence of increased number of TiO_2 active sites on the process kinetics; the photocatalytic degradation efficiency increased up to 60 mg L^{-1} and then declined with increasing catalyst loading.[158] Photodegradation of paracetamol using TiO_2 was also investigated by Desale *et al.* Degradation of paracetamol increased with increasing TiO_2 loading in the range 1 to 4 g L^{-1}. Catalyst loading of 1 g L^{-1} TiO_2 showed slow degradation of paracetamol. Catalyst loading of 2 g L^{-1} and 3 g L^{-1} TiO_2 had similar degradation. After 180 min, degradation of paracetamol in case of 2 g L^{-1} catalyst loading was more than that of 3 g L^{-1}. The 2 g L^{-1} TiO_2 catalyst loading showed remarkable degradation as compared to the 4 g L^{-1} loading. Based on the results, the optimum titanium dioxide concentration for degradation of paracetamol in aqueous solution was found to be 2 g L^{-1}.[159] Table 1 below shows the optimum concentration loading of different types of catalysts in a photocatalytic degradation system.

4.4.2 Effect of substrate concentration on photocatalytic systems for pharmaceutical waste treatment. The effect of substrate concentration plays a crucial role in the efficiency and kinetics of photocatalytic degradation.[82] Predominantly, at low concentrations of contaminants, the rate of degradation increases with increase in substrate concentration, since there are enough radicals and holes for reaction with contaminants. However, beyond the optimal concentration, the elimination efficiency decreases due to inadequate amount of hydroxyl radicals ($OH^{\bullet}$).[161] In addition, when concentration of contaminants increases, more active reactant species adhere to the surface of TiO_2, decreasing hydroxyl radical generation, as there are fewer specific sites for adhesion of hydroxyl anions. In addition, photons are absorbed by the contaminants before they can reach the catalyst surface, thus decreasing photocatalytic efficiency.[162]

The effect of substrate concentration on photodegradation by Degussa P25 was studied by Desale *et al.* using paracetamol as the substrate. It was observed that complete degradation of 50 mg L^{-1} of paracetamol was achieved at 90 min. The degradation rate depended on the initial concentration of paracetamol and decreases with increasing initial concentration of paracetamol. The degradation of paracetamol was found to be 100%, 80%, and 50% at an initial paracetamol concentration of 100, 200, and 500 mg L^{-1}, respectively, at 240 min. It was reported in the literature that photocatalytic reactions occur between the adsorbed substrate (paracetamol) and $OH^{\bullet}$ generated on TiO_2 surface. The concentration of adsorbed paracetamol increases with increase in initial paracetamol concentration.[159]

Ahmed and co-workers (2011)[124] studied photocatalytic decomposition influence of 2,4-dinitrophenol at an initial concentration of 10–76 ppm in the presence of TiO_2 and P25. It was noted that the highest decomposition was noted at 76 ppm. Comparable trends were studied for the photooxidation decomposition of erioglaucine, acephate, propachlor, phoshamidon, carbofuran, diphenamid and indole-3-buteric acid, as shown in Table 2 below.

4.4.3 pH effect on photocatalytic degradation in photocatalytic systems for pharmaceutical waste treatment. The pH of the solution is a paramount factor in photochemical reaction since it controls the size of the generated aggregates and the surface charge properties of the photocatalyst as well as dissolution and solubility.[26] At pH above pK_a value, hydrocarbon substances procure a negative charge, while below pK_a value, hydrocarbon substances maintain a neutral state. However, some substances may present in all charged and neutral forms in aqueous solution. These differences can thus greatly affect their photooxidation decomposition behavior. Depending on the pH, the following reactions (eqn (8) and (9)) are expected to take place on the surface of the catalyst:

$$TiOH + H^+ \rightarrow TiOH^{2+} \quad pK_{a1} \tag{8}$$

$$TiOH + OH^- \rightarrow TiO^- + H_2O \quad pK_{a2} \tag{9}$$

where K_a is the acid dissociation constant.

It can be seen that for pK_{a1}, the positive form of the TiO_2 surface rises as pH reduces; however, above pH 6, negative

Table 1 Optimum concentration loading of different types of catalysts in a photocatalytic degradation system

Type of catalyst	Optimum concentration loading (g l^{-1})	Ref.
Degussa P25	0.5–5	Bahenmaan *et al.*, (2007)[160] & Cao *et al.*, (2008)[116]
Chromotrope 2B/P25	0.5–5	Qamar *et al.*, (2015)[126]
Amido black 10B/P25	0.5–5	Qamar *et al.*, (2015)[118]
Orange G/P25	0.3–2	Zhang *et al.*, (2002)[45]

Table 2 Effect of different substrate concentrations on photocatalytic decomposition by UV/TiO_2 photocatalyst

Substrate	Photocatalyst	Optimum concentration (mM)	References
Phosphamidon	UV/TiO_2	0.46	Rahman and Muneer (2005)[122]
Acephate	UV/TiO_2	1.01	Rahman *et al.* (2006)[126]
Carbofuran	UV/TiO_2	0.08	Mahalakshmi *et al.* (2007)[146]
Erioglaucine	UV/TiO_2	0.007	Daneshvar *et al.* (2006)[117]
Prophachlor	UV/TiO_2	1.34	Muneer *et al.* (2005)[122]
Diphenamid	UV/TiO_2	0.59	Rahman *et al.* (2003)[126]
Indole-3-buteric acid	UV/TiO_2	0.29	Qamar and Muneer (2005)[120]

charges formed on the surface of TiO_2 increase with elevating pH (eqn (9)). This is because the pH of the solution influences the generation of OH radicals by kinetic interaction between OH^- ions and photogenerated holes on the TiO_2 surface. The cationic holes are deemed as the main contributors to photocatalytic steps at low pH, while $^{\bullet}OH$ radicals are regarded as the main particle at basic or neutral conditions.[163,164] Thus, when hydroxyl ions are available on the TiO_2 surface, the induction of $^{\bullet}OH$ increases, and hence, the efficiency of mineralization of pollutants is logically enhanced in neutral/basic condition, as shown in Fig. 4 below.

In order to further explain the influence of pH on photooxidation degradation of hydrocarbon substances and absorptivity on the TiO_2 surface, many investigations have been carried, out as shown in Table 3.

The effect of pH on aniline degradation rate was investigated in the range of 2–12 at aniline concentration of 50 mg L^{-1} and TiO_2 concentration of 60 mg L^{-1}. The aniline removal rates at different pH values at two different times of 60 and 120 min were compared. As the pH increased from acidic to alkaline, the rate of aniline removal efficiency increased and was maximum at pH 12. In case of initial pH values 2, 4, 6, 8, 10, and 12.0, the percentage removal of aniline was 27, 56, 62, 60, 66, and 76, and Kap was 0.128, 0.189, 0.265, 0.266, 0.304, and 0.45, respectively. The increasing aniline removal efficiency and Kap with increasing pH could be attributed to the increase in the number of OH^- ions at the surface of TiO_2 since OH^- can be formed by trapping photo-produced holes.[158]

4.4.4 Effect of electron acceptor on photocatalytic systems for pharmaceutical waste treatment. The charge carrier scavenger is one of the keys in fabricating future photocatalytic devices. Therefore, the introduction of the suitable electron acceptors to impede recombination of electron–hole pairs subsequently hinders quantum yield. Thus, the oxygen molecule is usually employed as an electron acceptor in photocatalysis. Inclusion of a foreign oxidant as electron acceptors in a semiconductor photocatalyst has been reported to enhance the decomposition rate of hydrocarbon pollutants as it enhances the scavenger effect by exciting electrons to the conduction band, proliferating $^{\bullet}OH$ radical concentration and oxidation rate of intermediate compounds and lastly generating more oxidizing species and radicals to hasten the decomposition of intermediate substances.[127,131,149] Researchers have investigated the influence of introducing various types of electron acceptors such as H_2O_2, $KBrO_3$, and $K_2S_2O_8$ on the photocatalytic decomposition activities on various contaminants[96,127] to improve the generation of $^{\bullet}OH$ radical scavenger effect. Most cases show that the introduction of oxidants results in better efficiency decomposition rate compared to molecular oxygen ($UV/TiO_2/BrO^{3-} > UV/TiO_2/S_2O_8^{2-} > UV/TiO_2/H_2O_2$). Improvement of decomposition rate is because of excitation of electrons from BrO^{3-} to the conduction band, which signifies a reduction in recombination of electron–hole pairs.[120] Fig. 5 shows the comparison of photocatalytic degradation rate of P25 in presence of different types of electron acceptors.

The addition of electron acceptors to the photodegradation mixture significantly enhances photodegradation rates of substrates. Paul *et al.* (2007)[167] observed a marked improvement in degradation of ciprofloxacin and other fluoroquinolones when bromate ion (BrO_3^-) was added as an electron acceptor. BrO_3^- promoted degradation when used in conjunction with visible light irradiation, whereas the absence of BrO_3^- or molecular oxygen (anaerobic conditions) prevented any significant photodegradation. Since the band gap energy of TiO_2 does not permit the formation of electron–hole pairs using visible light, it was suggested that photocatalytic oxidation of fluoroquinolones is mediated by the transfer of electron(s) to the electron acceptor, resulting in the formation of unstable radical fluoroquinolone species that are further oxidized.[168] Furthermore, the addition of hydroxyl radical scavengers (such as methanol) and superoxide scavengers (such as superoxide dismutase) decreased the degradation rate of ciprofloxacin under UV but not visible light irradiation. Such results suggested that visible-light-induced photocatalysis of ciprofloxacin is not mediated by electron–hole pairs as there are no significant changes to the photodegradation rate as a result of $HO^{\bullet}$ or $O_2^{\bullet}$ quenching. Diclofenac mineralization (*i.e.*, the complete conversion of the pharmaceutical to inorganic compounds such as CO_2, H_2O, and NH_3) improved with the addition of ozone to the UV/TiO_2 system and only 10% of the total organic carbon content (TOC) remained in the irradiated suspension compared with 30% TOC remaining in the absence of ozone. As TOC measures the concentration of parent pharmaceuticals and any intermediate photoproducts, the parameter is a

Table 3 Influence of pH on photocatalytic degradation

Substrate	Photocatalyst	Optimum pH	Ref.
Phorate	UV/TiO_2	8.1	Wu *et al.* (2009)[165]
Dimethoate	UV/TiO_2	11.00	Chen *et al.* (2007)[156]
Carbofuran	UV/TiO_2	6.9	Mahalakshmi *et al.* (2007)[146]
Carbendazim	UV/TiO_2	9.1	Saien and Khezrianjoo (2008)[166]

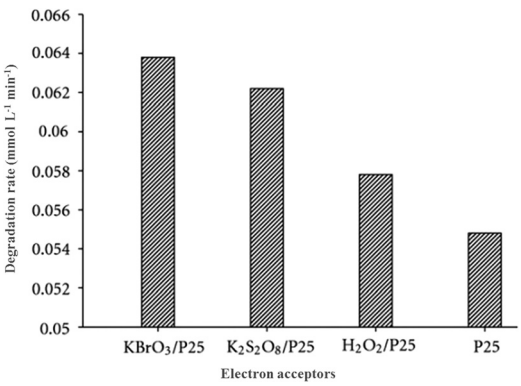

Fig. 5 Comparison of photocatalytic degradation rate of TiO_2-P25 in presence of different types of electron acceptors.[120]

good indicator of mineralization achieved by photocatalysis. Since the intermediate photoproducts formed *via* diclofenac photodegradation and photocatalysis were more toxic than the parent pharmaceutical, adding ozone improved the efficiency and acceptability of the UV/TiO_2 system as a feasible wastewater treatment process. However, the addition of a high concentration of H_2O_2 (>20 mmol L^{-1}) to a UV/TiO_2 photocatalytic fiber system inhibited the degradation of salicylic acid,[169] while lower H_2O_2 concentrations promoted salicylic acid degradation. It was suggested in the study that H_2O_2 may also act as an electron acceptor for conduction band electrons and may compete with molecular oxygen for adsorption sites on the surface of the TiO_2 photocatalyst.[11,168,170]

4.4.5 Effect of temperature on photocatalytic systems for pharmaceutical waste treatment. Mozia and co-workers (2015)[171] reported that increase in reaction temperature led to an increase in the photocatalytic decomposition rate in Acid Red. The study was evaluated under the influence of TiO_2 loadings at 0.3 and 0.5 g dm^{-3} with increment in solution temperature from 40 °C to 50 °C. Results showed when the temperature increased, a satisfactory degradation rate of 11% and 13% was observed under the effect of TiO_2 loadings. In addition, continuous increase in temperature to 60 °C displayed increment in the photocatalytic degradation rate by 10% addition on catalyst loadings. However, when the temperature reached 100 °C, the exothermic adsorption of reactant became adverse and hindered the reaction pathway.[69]

Besides, Soares and co-workers (2007)[172] investigated the influence of temperature on the reaction. Most favorable temperatures were found to be in the range 313 to 323 K, as shown in Fig. 6. At high temperature, sorption of the substances occurred to enhance the reaction because it is faster as compared to the decomposition on the surface and adhering of the reactants and dye on TiO_2. Matlack and Dicks (2015)[173] proposed that at higher temperatures, the decrease of adsorbed volume and decline in degradation rate are somewhat related to the amount of hydrocarbon and dissolved oxygen present.

The effect of temperature on aniline photodegradation in aqueous solution in the presence of TiO_2 and UV was investigated by Mansouri *et al.* in the range of 293–323 K. Increase in temperature from 293 to 323 K reduced the time required for aniline removal. For a removal of around 60%, for instance, the required time decreased from more than 120 min to about 30 min. Maximum aniline removal was determined to be 82% under irradiation of 2 h and temperature of 323 K. The reason for this observation is thought to be the fact that temperature is an important factor affecting adsorption and photocatalysis. In the case of photocatalysis, the photocatalytic degradation rate increases with increasing temperature.[158,166,174]

4.4.6 Effect of light intensity on photocatalytic systems for pharmaceutical waste treatment. The influence of ultra-violet and visible light irradiation time affects the decomposition of

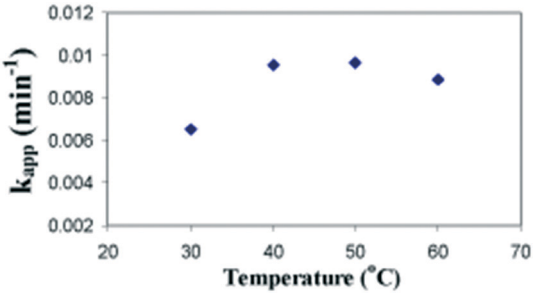

Fig. 6 Optimum temperature of a photocatalytic reaction ranging from 40 °C to 50 °C.[149]

dye in aqueous solution using a TiO_2 catalyst in a photocatalytic reactor. Ollis and co-workers (1992),[123] in agreement with Hussein,[150] stated that decomposition rate is directly proportional to increment in light intensity at low intensities (first kinetic order). However, beyond a certain irradiation value (approximately 25 mW cm^{-2}), the degradation rate depends on the square root of the light intensity (half order reaction). Lastly, at high intensities, the degradation rate does not depend on the light irradiation, as illustrated in Fig. 7. At this rate, the number of photons per unit time/unit area is high. Therefore, the probability of excitation of photons on the catalyst surface increases, thus increasing photocatalytic capacity.

Zhou and Wang[175] investigated the influence of irradiation intensity for decomposition of Orange G dye. The optimum degradation of pollutants was in the range of 215 to 586 μW cm^{-2}. On the other hand, Chanathaworn and colleagues (2012)[176] investigated light intensity of a blacklight lamp in the range of 0–114 W m^{-2} and evaluated the influence of light intensity on colour removal of Rhodamine B. Liu *et al.* (2006)[177] conducted a study at three different irradiation intensities (1.24 mW cm^{-2}, 2.04 mW m^{-2}, 3.15 mW m^{-2}) and noted that increasing irradiation intensities aids in colour removal of Acid Yellow 17. All three studies agree that increase in irradiation intensity improves dye decolorization rate.[87]

Diclofenac (DCF), a widely used non-steroidal anti-inflammatory drug (NSAID), is a commonly detected substance in

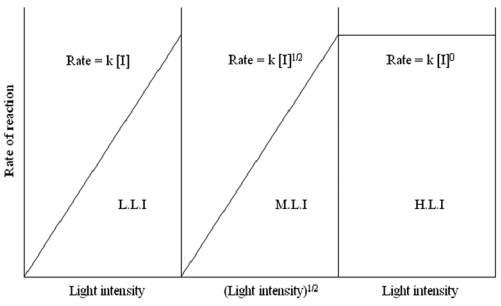

Fig. 7 Impact of light intensity from low light intensity (leftmost) to highest light intensity (rightmost) on kinetics of photocatalytic degradation.[124]

wastewater. There is no evidence of a true kinetic study on photocatalytic degradation of DCF with respect to light intensity. Therefore, a thorough investigation of rates corresponding to different radiant flux in the range of 14–45 W m^{-2} was conducted by Hashim *et al.*[178] Fig. 8 shows these results. The kinetic constant can be related to the light intensity according to the following expression:

$$kr = \alpha(I)\,\beta \tag{10}$$

A value of 0.53 was found for β and 0.9243 for α. Previous studies on semiconductor photocatalysis of organic compounds with respect to light intensity indicated that reaction rate increases with the square root of light intensity at high intensities. On the other hand, at low levels of illumination, degradation rate was observed to be 75 with respect to intensity. In this study, however, a trend close to a square root relationship was observed.[178,179]

5.0 Kinetics studies on photodegradation of pharmaceutical pollutants

5.1 First order kinetics

The mechanism of heterogeneous photocatalysis has been studied by many researchers in terms of Langmuir–Hinshelwood (L–H) rate equations. This is because photocatalytic oxidation produces a series of steps that result in successive adsorption and degradation under illumination by visible light.[180] The first order kinetics has been proved by Liao and co-workers on investigation of photocatalytic degradation by studying the effect of initial concentration of organic contaminants and the results are compatible with the first order kinetics model.[181]

The kinetics of photodegradation rate of most organic contaminants can be well described by pseudo-first order kinetics. Integration of this equation (with the same conditions of $C = C_0$ at $t = 0$, with C_0 being the initial concentration in the bulk solution, C is the amount of concentration, t is reaction time and k is the reaction rate constant) will lead to the expected relations (eqn (11) and (12)):[182]

$$\mathrm{DG} = -\frac{\mathrm{d}C}{\mathrm{d}t} = kC \tag{11}$$

$$\int_{C_0}^{c} -\mathrm{d}C = k\int_0^t \mathrm{d}t$$

$$\ln\frac{C_0}{C} = kt \tag{12}$$

From the above equations, L–H equation for photocatalytic degradation can be determined by plotting the reciprocal of rate constant ($1/k$) against initial dye concentration C_0, as shown in Fig. 9.

5.2 Second order kinetics

Isotherm modeling generally contemplates interaction between organic substrate and photocatalyst until a state of equilibrium is achieved. In order to optimize the effectiveness of TiO_2/silica in photodegradation of methyl orange, linear form of Langmuir and Freundlich models is applied for the TiO_2/silica composite photocatalyst, and pseudo-first order equations are generalized to two-site-occupancy adsorption to form a pseudo-second order equation as below (where k_2 represents pseudo-second order rate constant, q_e represent dye concentration at equilibrium onto absorbent).[184]

$$\frac{t}{C_t} = \frac{1}{k_2 q_e^{\,2}} + \frac{t}{q_e} \tag{13}$$

According to Pete (2015),[133] the pseudo-second order model enables estimation of experimental q_e values effectively and is less sensitive in detecting random errors. An experiment has been conducted by Yang and colleagues on kinetic mechanism of photocatalytic degradation of various organic compounds on modified TiO_2/activated carbon composite photocatalyst. Results show that toluene and acetone were deduced to be fitted with the second order mechanism.

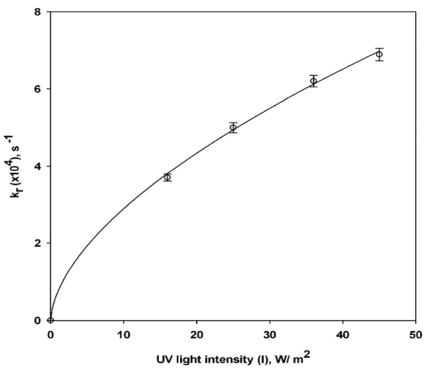

Fig. 8 Effect of light intensity on the degradation rate of DCF. Experimental conditions: $Q = 1.15 \times 10^{-5}$ m^3 s^{-1}, VL = 4×10^{-4} m^3, $[DCF]_o$ = 25 ppm, T = 298 K, O_2 saturated.

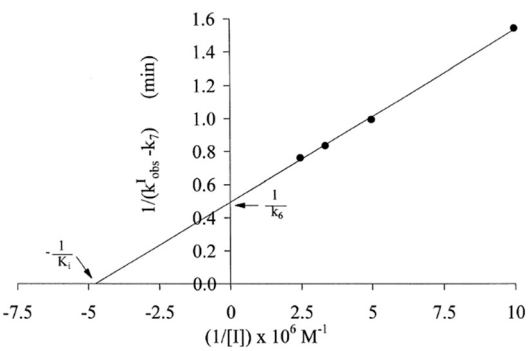

Fig. 9 Linear reciprocal of rate constant *versus* initial dye concentrations.[183]

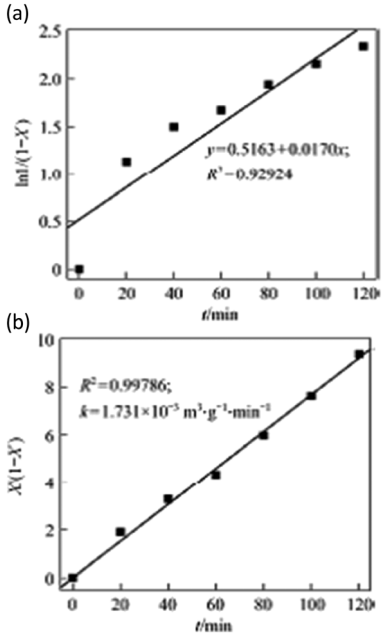

Fig. 10 (a) Pseudo-first order and (b) pseudo-second order kinetic model of photocatalytic reaction in toluene.[185]

When the initial concentration of toluene increases, the second order kinetic rate constant increases rapidly.[185] The validity of the kinetic model is partly proved by plotting the experimental data obtained in first and second order kinetic expressions under various conditions, as shown in Fig. 10.

Conclusions

Photocatalysis is a propitious technique for the elimination of emerging contaminants. However, the application of ultraviolet light in large-scale plants for treatment of huge quantities of effluents is not feasible or economical. Among semiconductors, TiO_2 has been recognized for its capacity to absorb a wide range of light spectrum at a threshold of 425 nm. The use of modified TiO_2 catalyst that can exploit UV/visible/solar irradiation produces a promising and sustainable process. However, numerous parameters such as catalyst dosage, pollutant concentration, pH and refinement of the photocatalyst (doping or heterojunction of semiconductor/nanomaterial) should be considered and optimized for an efficient removal process. Most current literature deals with commercial types of TiO_2, especially for dye removal, and photocatalytic behavior in the degradation of emerging contaminants such as pharmaceutical compounds has been scarcely investigated or reported. Besides the optimization of governing parameters for their impact on degradation processes and the modifications of TiO_2 catalyst, other factors such as the introduction of ultrasound irradiation and electron acceptors into the solution may considerably improve the efficiency of the photocatalytic degradation. Considering that the generated by-products may be more hazardous than the parent compounds, the evaluation of total organic pollutant (TOP) removal in the process is crucial. Thus, various techniques yielding visible-light-driven photocatalysts with improved photocatalytic activity can be focused either on narrowing the band gap of the photocatalyst or improving charge separation. The recently achieved progress in this field indicates that the application of visible-light-driven photocatalysts is a potential method to treat antibiotic wastewater. Large-scale production of photocatalysts is necessary to realize commercial application of photocatalysis in treating antibiotic waste. Therefore, the development of simple and effective methods for large-scale preparation is key to photocatalyst application in future.

Conflicts of interest

There are no conflicts to declare.

Acknowledgements

This work was supported by the Natural Science and Engineering Research Council of Canada (NSERC) through the Strategic Project (SP) and Discovery Grants. The author would like to thank EXP Inc. and SiliCycle Inc. for their support.

References

1 S. K. Khetan and T. J. Collins, *Chem. Rev.*, 2007, **107**, 2319–2364.
2 S. Malato, P. Fernández-Ibáñez, M. I. Maldonado, J. Blanco and W. Gernjak, *Catal. Today*, 2009, **147**, 1–59.
3 B. Razavi, S. B. Abdelmelek, W. Song, K. E. O'Shea and W. J. Cooper, *Water Res.*, 2011, **45**, 625–631.
4 H. Xu, W. J. Cooper, J. Jung and W. Song, *Water Res.*, 2011, **45**, 632–638.
5 L. Carlos, B. W. Pedersen, P. R. Ogilby and D. O. Mártire, *Photochem. Photobiol. Sci.*, 2011, **10**, 1080–1086.
6 L. Carlos, D. O. Mártire, M. C. Gonzalez, J. Gomis, A. Bernabeu, A. M. Amat and A. Arques, *Water Res.*, 2012, **46**, 4732–4740.
7 M. L. Marin, L. Santos-Juanes, A. Arques, A. M. Amat and M. A. Miranda, *Chem. Rev.*, 2011, **112**, 1710–1750.
8 J. V. Goldstone and B. M. Voelker, *Environ. Sci. Technol.*, 2000, **34**, 1043–1048.
9 A. Paul, S. Hackbarth, R. D. Vogt, B. Röder, B. K. Burnison and C. E. Steinberg, *Photochem. Photobiol. Sci.*, 2004, **3**, 273–280.
10 J. Schwaiger, H. Ferling, U. Mallow, H. Wintermayr and R. Negele, *Aquat. Toxicol.*, 2004, **68**, 141–150.
11 F. Méndez-Arriaga, S. Esplugas and J. Giménez, *Water Res.*, 2008, **42**, 585–594.
12 T. Mahmud, S. S. Rafi, D. L. Scott, J. M. Wrigglesworth and I. Bjarnason, *Arthritis Rheum.*, 1996, **39**, 1998–2003.
13 S. K. Samanta, O. V. Singh and R. K. Jain, *Trends Biotechnol.*, 2002, **20**, 243–248.
14 E. Bååth, M. Díaz-Raviña, Å. Frostegård and C. D. Campbell, *Appl. Environ. Microbiol.*, 1998, **64**, 238–245.
15 V. M. A. Calisto, *Environmental occurrence and fate of psychiatric pharmaceuticals*, 2011.

16 R. Shetty, V. B. Chavan, P. S. Kulkarni, B. D. Kulkarni and S. P. Kamble, *Indian Chem. Eng.*, 2016, 1–23.
17 M. O. Awaleh and Y. D. Soubaneh, *Hydrol.: Curr. Res.*, 2014, **5**, 1–12.
18 U. I. Gaya and A. H. Abdullah, *J. Photochem. Photobiol., C*, 2008, **9**, 1–12.
19 W. Zhu, *et al.*, *Appl. Catal., B*, 2017, **207**, 93–102.
20 J. Liu, H. Bai, Y. Wang, Z. Liu, X. Zhang and D. D. Sun, *Adv. Funct. Mater.*, 2010, **20**, 4175–4181.
21 C. M. Teh and A. R. Mohamed, *J. Alloys Compd.*, 2011, **509**, 1648–1660.
22 D. Beydoun, R. Amal, G. Low and S. McEvoy, *J. Nanopart. Res.*, 1999, **1**, 439–458.
23 Y. J. Hwang, C. Hahn, B. Liu and P. Yang, *ACS Nano*, 2012, **6**, 5060–5069.
24 S. Rehman, R. Ullah, A. Butt and N. Gohar, *J. Hazard. Mater.*, 2009, **170**, 560–569.
25 M. Rauf, M. Meetani and S. Hisaindee, *Desalination*, 2011, **276**, 13–27.
26 M. Sioi, A. Bolosis, E. Kostopoulou and I. Poulios, Photocatalytic treatment of colored wastewater from medical laboratories: photocatalytic oxidation of hematoxylin, *J. Photochem. Photobiol., A*, 2006, **184**(1–2), 18–25.
27 R. Daghrir, P. Drogui and D. Robert, *Ind. Eng. Chem. Res.*, 2013, **52**, 3581–3599.
28 A. O. Ibhadon and P. Fitzpatrick, *Catalysts*, 2013, **3**, 189–218.
29 S. Morales-Torres, L. M. Pastrana-Martínez, J. L. Figueiredo, J. L. Faria and A. M. Silva, *Appl. Surf. Sci.*, 2013, **275**, 361–368.
30 S. Canonica, *Chimia*, 2007, **61**, 641–644.
31 J. J. Pignatello, E. Oliveros and A. MacKay, *Crit. Rev. Environ. Sci. Technol.*, 2006, **36**, 1–84.
32 C. Ratanatawanate, *et al.*, *J. Phys. Chem. C*, 2011, **115**(14), 6175–6180.
33 E. Montoneri, L. Tomasso, N. Colajanni, I. Zelano, F. Alberi, G. Cossa and R. Barberis, *Int. J. Environ. Sci. Technol.*, 2014, **11**, 251–262.
34 S.-F. Yang, *et al.*, Sorption and biodegradation of sulfonamide antibiotics by activated sludge: experimental assessment using batch data obtained under aerobic conditions, *Water Res.*, 2011, **45**(11), 3389–3397.
35 P. C. Lindholm-Lehto, H. S. Ahkola, J. S. Knuutinen and S. H. Herve, *Environ. Sci. Pollut. Res.*, 2016, **23**, 7985–7997.
36 Y. Im, S. Kang, K. M. Kim, T. Ju, G. B. Han, N.-K. Park, T. J. Lee and M. Kang, *Int. J. Photoenergy*, 2013, **2013**, 452542.
37 G. Magnacca, E. Laurenti, E. Vigna, F. Franzoso, L. Tomasso, E. Montoneri and V. Boffa, *Process Biochem.*, 2012, **47**, 2025–2031.
38 P. Avetta, A. B. Prevot, D. Fabbri, E. Montoneri and L. Tomasso, *Chem. Eng. J.*, 2012, **197**, 193–198.
39 A. Bianco Prevot, P. Avetta, D. Fabbri, E. Laurenti, T. Marchis, D. G. Perrone, E. Montoneri and V. Boffa, *ChemSusChem*, 2011, **4**, 85–90.
40 A. B. Prevot, D. Fabbri, E. Pramauro, C. Baiocchi, C. Medana, E. Montoneri and V. Boffa, *J. Photochem. Photobiol., A*, 2010, **209**, 224–231.
41 J. Gomis, R. Vercher, A. Amat, D. Mártire, M. González, A. B. Prevot, E. Montoneri, A. Arques and L. Carlos, *Catal. Today*, 2013, **209**, 176–180.
42 K. E. Murray, S. M. Thomas and A. A. Bodour, *Environ. Pollut.*, 2010, **158**, 3462–3471.
43 S. D. Richardson, *Anal. Chem.*, 2008, **80**, 4373–4402.
44 M. Klavarioti, D. Mantzavinos and D. Kassinos, *Environ. Int.*, 2009, **35**, 402–417.
45 J. Shen, Y.-n. Wu, L. Fu, B. Zhang and F. Li, *J. Mater. Sci.*, 2014, **49**, 2303–2314.
46 E. M. Brazón, C. Piccirillo, I. Moreira and P. Castro, *J. Environ. Manage.*, 2016, **182**, 486–495.
47 F. Martínez, M. López-Muñoz, J. Aguado, J. Melero, J. Arsuaga, A. Sotto, R. Molina, Y. Segura, M. Pariente and A. Revilla, *Water Res.*, 2013, **47**, 5647–5658.
48 D. Hernández-Uresti, A. Vázquez, D. Sanchez-Martinez and S. Obregón, *J. Photochem. Photobiol., A*, 2016, **324**, 47–52.
49 A. Mellouki, T. Wallington and J. Chen, *Chem. Rev.*, 2015, **115**, 3984–4014.
50 D. Zhang, G. Luo, X. Ding and C. Lu, *Acta Pharm. Sin. B*, 2012, **2**, 549–561.
51 G. Williams, B. Seger and P. V. Kamat, TiO_2-graphene nanocomposites. UV-assisted photocatalytic reduction of graphene oxide, *ACS Nano*, 2008, **2**(7), 1487–1491.
52 D. Bahnemann, *Sol. Energy*, 2004, **77**, 445–459.
53 A. Kubacka, M. Fernández-García and G. Colón, *Chem. Rev.*, 2012, **112**, 1555–1614.
54 E. Luévano-Hipólito, A. Martínez-de la Cruz and E. L. Cuéllar, *J. Taiwan Inst. Chem. Eng.*, 2014, **45**, 2749–2754.
55 X. Wang, K. Maeda, A. Thomas, K. Takanabe, G. Xin, J. M. Carlsson, K. Domen and M. Antonietti, *Nat. Mater.*, 2009, **8**, 76–80.
56 A. Thomas, A. Fischer, F. Goettmann, M. Antonietti, J.-O. Müller, R. Schlögl and J. M. Carlsson, *J. Mater. Chem.*, 2008, **18**, 4893–4908.
57 F. Dong, L. Wu, Y. Sun, M. Fu, Z. Wu and S. Lee, *J. Mater. Chem.*, 2011, **21**, 15171–15174.
58 S. Yang, Y. Gong, J. Zhang, L. Zhan, L. Ma, Z. Fang, R. Vajtai, X. Wang and P. M. Ajayan, *Adv. Mater.*, 2013, **25**, 2452–2456.
59 V. L. Cunningham, S. P. Binks and M. J. Olson, *Regul. Toxicol. Pharmacol.*, 2009, **53**, 39–45.
60 X.-H. Li, J.-S. Chen, X. Wang, J. Sun and M. Antonietti, *J. Am. Chem. Soc.*, 2011, **133**, 8074–8077.
61 Y. Tao, Q. Ni, M. Wei, D. Xia, X. Li and A. Xu, *RSC Adv.*, 2015, **5**, 44128–44136.
62 C. Miranda, H. Mansilla, J. Yáñez, S. Obregón and G. Colón, *J. Photochem. Photobiol., A*, 2013, **253**, 16–21.
63 M. Trapido, I. Epold, J. Bolobajev and N. Dulova, *Environ. Sci. Pollut. Res.*, 2014, **21**, 12217–12222.
64 J. Araña, J. Doña-Rodríguez, D. Portillo-Carrizo, C. Fernández-Rodríguez, J. Pérez-Peña, O. G. Díaz, J. Navío and M. Macías, *Appl. Catal., B*, 2010, **100**, 346–354.
65 E. Seck, J. Doña-Rodríguez, C. Fernández-Rodríguez, O. González-Díaz, J. Arana and J. Pérez-Peña, *Appl. Catal., B*, 2012, **125**, 28–34.

66 E. Seck, J. Doña-Rodríguez, C. Fernández-Rodríguez, O. González-Díaz, J. Araña and J. Pérez-Peña, *Chem. Eng. J.*, 2012, **203**, 52–62.
67 E. Seck, J. Doña-Rodríguez, C. Fernández-Rodríguez, D. Portillo-Carrizo, M. Hernández-Rodríguez, O. González-Díaz and J. Pérez-Peña, *Sol. Energy*, 2013, **87**, 150–157.
68 L. Prieto-Rodriguez, S. Miralles-Cuevas, I. Oller, A. Agüera, G. L. Puma and S. Malato, *J. Hazard. Mater.*, 2012, **211**, 131–137.
69 X. An, H. Liu, J. Qu, S. J. Moniz and J. Tang, *New J. Chem.*, 2015, **39**, 314–320.
70 C. Y. Park, *et al.*, Preparation of novel CdS-graphene/TiO_2 composites with high photocatalytic activity for methylene blue dye under visible light, *Bull. Mater. Sci.*, 2013, **36**(5), 869–876.
71 Y. Fan, *et al.*, An overview on water splitting photocatalysts, *Front. Chem. China*, 2009, **4**(4), 343–351.
72 O. Gimeno, M. Carbajo, F. J. Beltrán and F. J. Rivas, *J. Hazard. Mater.*, 2005, **119**, 99–108.
73 L. Li, *et al.*, *J. Phys. Chem. C*, 2014, **118**(30), 16526–16535.
74 M. R. Hoffmann, S. T. Martin, W. Choi and D. W. Bahnemann, *Chem. Rev.*, 1995, **95**, 69–96.
75 B. Priya, P. Raizada, N. Singh, P. Thakur and P. Singh, *J. Colloid Interface Sci.*, 2016, **479**, 271–283.
76 S. Ahmed, M. Rasul, R. Brown and M. Hashib, *J. Environ. Manage.*, 2011, **92**, 311–330.
77 M. A. Fox and M. T. Dulay, *Chem. Rev.*, 1993, **93**, 341–357.
78 A. L. Linsebigler, G. Lu and J. T. Yates Jr, *Chem. Rev.*, 1995, **95**, 735–758.
79 M. Długosz, P. Żmudzki, A. Kwiecień, K. Szczubiałka, J. Krzek and M. Nowakowska, *J. Hazard. Mater.*, 2015, **298**, 146–153.
80 M. Anpo and M. Takeuchi, *J. Catal.*, 2003, **216**, 505–516.
81 J. C. Yu, W. Ho, J. Yu, H. Yip, P. K. Wong and J. Zhao, *Environ. Sci. Technol.*, 2005, **39**, 1175–1179.
82 N. Shi, R. Yan, H. Zhou, D. Zhang and T. Fan, *Curr. Org. Chem.*, 2015, **19**, 521–539.
83 M. Tokumura, A. Sugawara, M. Raknuzzaman, M. Habibullah-Al-Mamun and S. Masunaga, *Chemosphere*, 2016, **159**, 317–325.
84 A. Khataee, M.-N. Pons and O. Zahraa, *J. Hazard. Mater.*, 2009, **168**, 451–457.
85 X. Zhang and L. Lei, *J. Hazard. Mater.*, 2008, **153**, 827–833.
86 S. Carbonaro, M. N. Sugihara and T. J. Strathmann, *Appl. Catal., B*, 2013, **129**, 1–12.
87 S. Sakthivel, B. Neppolian, M. Shankar, B. Arabindoo, M. Palanichamy and V. Murugesan, *Sol. Energy Mater. Sol. Cells*, 2003, **77**, 65–82.
88 C. So, M. Y. Cheng, J. Yu and P. Wong, *Chemosphere*, 2002, **46**, 905–912.
89 C. C. de Escobar, M. A. Lansarin and J. H. Z. dos Santos, *J. Hazard. Mater.*, 2016, **306**, 359–366.
90 P. M. Álvarez, J. Jaramillo, F. Lopez-Pinero and P. K. Plucinski, *Appl. Catal., B*, 2010, **100**, 338–345.
91 L. Feng, E. D. van Hullebusch, M. A. Rodrigo, G. Esposito and M. A. Oturan, *Chem. Eng. J.*, 2013, **228**, 944–964.
92 E. B. Simsek, *Appl. Catal., B*, 2017, **200**, 309–322.
93 M. Ahmadi, H. R. Motlagh, N. Jaafarzadeh, A. Mostoufi, R. Saeedi, G. Barzegar and S. Jorfi, *J. Environ. Manage.*, 2017, **186**, 55–63.
94 A. Mirzaei, Z. Chen, F. Haghighat and L. Yerushalmi, *Sustain. Cities Soc.*, 2016, **27**, 407–418.
95 C. Guillard, H. Lachheb, A. Houas, M. Ksibi, E. Elaloui and J.-M. Herrmann, *J. Photochem. Photobiol., A*, 2003, **158**, 27–36.
96 T. Sauer, G. C. Neto, H. Jose and R. Moreira, *J. Photochem. Photobiol., A*, 2002, **149**, 147–154.
97 Y. Parent, D. Blake, K. Magrini-Bair, C. Lyons, C. Turchi, A. Watt, E. Wolfrum and M. Prairie, *Sol. Energy*, 1996, **56**, 429–437.
98 H. Choi, S. R. Al-Abed, D. D. Dionysiou, E. Stathatos and P. Lianos, *Sustainability science and engineering*, 2010, vol. 2, pp. 229–254.
99 K. M. Lee, C. W. Lai, K. S. Ngai and J. C. Juan, *Water Res.*, 2016, **88**, 428–448.
100 G. Tian, H. Fu, L. Jing, B. Xin and K. Pan, *J. Phys. Chem. C*, 2008, **112**, 3083–3089.
101 M. A. Lazar, S. Varghese and S. S. Nair, *Catalysts*, 2012, **2**, 572–601.
102 C. Singh, R. Chaudhary and R. S. Thakur, *Int. J. Energy Environ.*, 2011, **2**, 337–350.
103 H. Gulyas, *J. Adv. Chem. Eng.*, 2014, **4**(2), 1000108.
104 S. Kumar, W. Ahlawat, G. Bhanjana, S. Heydarifard, M. M. Nazhad and N. Dilbaghi, *J. Nanosci. Nanotechnol.*, 2014, **14**, 1838–1858.
105 J. C. Yu, J. Yu, W. Ho, Z. Jiang and L. Zhang, *Chem. Mater.*, 2002, **14**, 3808–3816.
106 M. N. Chong, B. Jin, C. W. Chow and C. Saint, *Water Res.*, 2010, **44**, 2997–3027.
107 X. Qu, P. J. Alvarez and Q. Li, *Water Res.*, 2013, **47**, 3931–3946.
108 E. Serrano, G. Rus and J. Garcia-Martinez, *Renewable Sustainable Energy Rev.*, 2009, **13**, 2373–2384.
109 V. Likodimos, D. D. Dionysiou and P. Falaras, *Rev. Environ. Sci. Bio/Technol.*, 2010, **9**, 87–94.
110 S. Devipriya and S. Yesodharan, *Sol. Energy Mater. Sol. Cells*, 2005, **86**, 309–348.
111 E. Forgacs, T. Cserhati and G. Oros, *Environ. Int.*, 2004, **30**, 953–971.
112 K.-H. Wang, Y.-H. Hsieh, M.-Y. Chou and C.-Y. Chang, *Appl. Catal., B*, 1999, **21**, 1–8.
113 M. Barakat, *Arabian J. Chem.*, 2011, **4**, 361–377.
114 J.-M. Herrmann, *Catal. Today*, 1999, **53**, 115–129.
115 W. Bahnemann, M. Muneer and M. Haque, *Catal. Today*, 2007, **124**, 133–148.
116 Y. Cao, H. Tan, T. Shi, T. Tang and J. Li, *J. Chem. Technol. Biotechnol.*, 2008, **83**, 546–552.
117 N. Daneshvar, D. Salari, A. Niaei and A. Khataee, *J. Environ. Sci. Health, Part B*, 2006, **41**, 1273–1290.
118 M. Muneer, M. Qamar, M. Saquib and D. Bahnemann, *Chemosphere*, 2005, **61**, 457–468.
119 M. Muneer and D. Bahnemann, *Appl. Catal., B*, 2002, **36**, 95–111.

120 M. Qamar and M. Muneer, *J. Hazard. Mater.*, 2005, **120**, 219–227.
121 M. A. Rahman and M. Muneer, *J. Environ. Sci. Health, Part B*, 2005, **40**(2), 247–267.
122 M. A. Rahman and M. Muneer, *Desalination*, 2005, **181**, 161–172.
123 D. F. Ollis, E. Pelizzetti and N. Serpone, Photocatalyzed destruction of water contaminants, *Environ. Sci. Technol.*, 1991, **25**(9), 1522–1529.
124 S. Ahmed, M. Rasul, W. N. Martens, R. Brown and M. Hashib, *Water, Air, Soil Pollut.*, 2011, **215**, 3–29.
125 H. K. Singh, M. Saquib, M. M. Haque, M. Muneer and D. W. Bahnemann, *J. Mol. Catal. A: Chem.*, 2007, **264**, 66–72.
126 A. M. Rahman, M. Qamar, M. Muneer and D. Bahnemann, *J. Adv. Oxid. Technol.*, 2006, **9**, 103–109.
127 Y. C. Zhang, Z. N. Du, K. W. Li, M. Zhang and D. D. Dionysiou, *ACS Appl. Mater. Interfaces*, 2011, **3**, 1528–1537.
128 N. Klamerth, S. Malato, M. Maldonado, A. Aguera and A. Fernández-Alba, *Environ. Sci. Technol.*, 2010, **44**, 1792–1798.
129 L. Lin, H. Wang, W. Jiang, A. R. Mkaouar and P. Xu, *J. Hazard. Mater.*, 2017, **333**, 162–168.
130 Z. Wu, F. Dong, W. Zhao, H. Wang, Y. Liu and B. Guan, *Nanotechnology*, 2009, **20**, 235701.
131 W. Yi, C. Yan, J. Ma, J. Xiong and H. Zhang, 2016.
132 H. Koohestani and S. K. Sadrnezhaad, *Desalin. Water Treat.*, 2016, **57**, 22029–22038.
133 K. Y. Pete, Photocatalytic degradation of dyes and pesticides in the presence of ions, *Dissertation*, Department of Chemical Engineering, Faculty of Engineering and Technology, Vaal University of Technology, 2015, http://digiresearch.vut.ac.za/handle/10352/308.
134 Y. Bi, H. Hu, S. Ouyang, Z. Jiao, G. Lu and J. Ye, Selective growth of Ag_3PO_4 submicro-cubes on Ag nanowires to fabricate necklace-like heterostructures for photocatalytic applications, *J. Mater. Chem.*, 2012, **22**, 14847–14850.
135 C. Liu, D. Yang, Y. Jiao, Y. Tian, Y. Wang and Z. Jiang, *ACS Appl. Mater. Interfaces*, 2013, **5**, 3824–3832.
136 S. Liu, N. Zhang, Z.-R. Tang and Y.-J. Xu, *ACS Appl. Mater. Interfaces*, 2012, **4**, 6378–6385.
137 H. Wang, Z. Wu and Y. Liu, *J. Phys. Chem. C*, 2009, **113**, 13317–13324.
138 F. Dong, H. Wang and Z. Wu, *J. Phys. Chem. C*, 2009, **113**, 16717–16723.
139 C.-Y. Yen, Y.-F. Lin, C.-H. Hung, Y.-H. Tseng, C.-C. M. Ma, M.-C. Chang and H. Shao, *Nanotechnology*, 2008, **19**, 045604.
140 D.-Y. Wang, M. Gong, H.-L. Chou, C.-J. Pan, H.-A. Chen, Y. Wu, M.-C. Lin, M. Guan, J. Yang and C.-W. Chen, *J. Am. Chem. Soc.*, 2015, **137**, 1587–1592.
141 Y.-J. Xu, Y. Zhuang and X. Fu, *J. Phys. Chem. C*, 2010, **114**, 2669–2676.
142 Y. Yao, G. Li, S. Ciston, R. M. Lueptow and K. A. Gray, *Environ. Sci. Technol.*, 2008, **42**, 4952–4957.
143 J. Zhang, M. Zhang, C. Yang and X. Wang, *Adv. Mater.*, 2014, **26**, 4121–4126.
144 G. Hu, X. Meng, X. Feng, Y. Ding, S. Zhang and M. Yang, *J. Mater. Sci.*, 2007, **42**, 7162–7170.
145 M. Khraisheh, J. Kim, L. Campos, H. Ala'a, A. Al-Hawari, M. Al Ghouti and G. M. Walker, *J. Ind. Eng. Chem.*, 2014, **20**, 979–987.
146 M. Mahalakshmi, B. Arabindoo, M. Palanichamy and V. Murugesan, *J. Hazard. Mater.*, 2007, **143**, 240–245.
147 C. Andriantsiferana, E. F. Mohamed and H. Delmas, *Environ. Technol.*, 2014, **35**, 355–363.
148 D. Mijin, J. Radivojević and P. Jovančić, *Chem. Ind. Chem. Eng. Q.*, 2007, **13**, 33–37.
149 E. T. Soares, M. A. Lansarin and C. C. Moro, *Braz. J. Chem. Eng.*, 2007, **24**, 29–36.
150 F. H. Hussein, *Asian J. Chem.*, 2012, **24**, 5427.
151 X.-j. Wang, W.-y. Yang, F.-t. Li, Y.-b. Xue, R.-h. Liu and Y.-j. Hao, *Ind. Eng. Chem. Res.*, 2013, **52**, 17140–17150.
152 A. Di Paola, E. García-López, G. Marcì and L. Palmisano, *J. Hazard. Mater.*, 2012, **211**, 3–29.
153 X. Zhang, L. Yu, C. Zhuang, T. Peng, R. Li and X. Li, *ACS Catal.*, 2013, **4**, 162–170.
154 Y. T. Liang, B. K. Vijayan, O. Lyandres, K. A. Gray and M. C. Hersam, *J. Phys. Chem. Lett.*, 2012, **3**, 1760–1765.
155 Y. Zhang, Z.-R. Tang, X. Fu and Y.-J. Xu, *ACS Nano*, 2010, **4**, 7303–7314.
156 K. Wang, J. Chen, Z. Zeng, J. Tarr, W. Zhou, Y. Zhang, Y. Yan, C. Jiang, J. Pern and A. Mascarenhas, *Appl. Phys. Lett.*, 2010, **96**, 123105.
157 M. Neamțu, D. Grandjean, A. Sienkiewicz, S. Le Faucheur, V. Slaveykova, J. J. V. Colmenares, C. Pulgarín and L. F. de Alencastro, *Appl. Catal., B*, 2014, **158**, 30–37.
158 F. Shahrezaei, *et al.*, Photocatalytic degradation of aniline using TiO_2 nanoparticles in a vertical circulating photocatalytic reactor, *Int. J. Photoenergy*, 2012, **2012**, 430638.
159 A. Desale, S. P. Kamble and M. P. Deosarkar, *Int. J. Chem. Phys. Sci.*, 2013, **2**, 140–148.
160 W. Raza, *et al.*, Synthesis of visible light driven TiO_2 coated carbon nanospheres for degradation of dyes, *Arabian J. Chem.*, 2015, DOI: 10.1016/j.arabjc.2015.09.002.
161 J. Ding, Z. Dai, F. Qin, H. Zhao, S. Zhao and R. Chen, *Appl. Catal., B*, 2017, **205**, 281–291.
162 S. Chen and Y. Liu, *Chemosphere*, 2007, **67**, 1010–1017.
163 M. Ogawa and K. Kuroda, *Chem. Rev.*, 1995, **95**, 399–438.
164 N. Talebian, S. M. Amininezhad and M. Doudi, *J. Photochem. Photobiol., B*, 2013, **120**, 66–73.
165 S. Wang, D. Mao, X. Guo, G. Wu and G. Lu, *Catal. Commun.*, 2009, **10**, 1367–1370.
166 J. Saien and S. Khezrianjoo, *J. Hazard. Mater.*, 2008, **157**, 269–276.
167 T. Paul, P. L. Miller and T. J. Strathmann, *Environ. Sci. Technol.*, 2007, **41**, 4720–4727.
168 A. Y. C. Tong, R. Braund, D. S. Warren and B. M. Peake, *Cent. Eur. J. Chem.*, 2012, **10**, 989–1027.
169 G. Laera, B. Jin, H. Zhu and A. Lopez, *Catal. Today*, 2011, **161**, 147–152.
170 M. Piecha, M. Sarakha and P. Trebše, *J. Photochem. Photobiol., A*, 2010, **213**, 61–69.

171 J. Kapica-Kozar, E. Kusiak-Nejman, A. Wanag, Ł. Kowalczyk, R. J. Wrobel, S. Mozia and A. W. Morawski, *Microporous Mesoporous Mater.*, 2015, **202**, 241–249.
172 P. Soares, A. Mikowski, C. M. Lepienski, E. Santos, G. A. Soares and N. K. Kuromoto, *J. Biomed. Mater. Res., Part B*, 2008, **84**, 524–530.
173 A. S. Matlack and A. P. Dicks, *Problem-Solving Exercises in Green and Sustainable Chemistry*, CRC Press, 2015.
174 L. Sanchez, J. Peral and X. Domenech, *Electrochim. Acta*, 1997, **42**, 1877–1882.
175 W. Zhou, H. Liu, J. Wang, D. Liu, G. Du and J. Cui, *ACS Appl. Mater. Interfaces*, 2010, **2**, 2385–2392.
176 J. Chanathaworn, C. Bunyakan, W. Wiyaratn and J. Chungsiriporn, *Songklanakarin J. Sci. Technol.*, 2012, **34**, 203.
177 H. G. Yang, C. H. Sun, S. Z. Qiao, J. Zou, G. Liu, S. C. Smith, H. M. Cheng and G. Q. Lu, *Nature*, 2008, **453**, 638–641.
178 N. Hashim, Visible Light Driven Photocatalysis, *PhD thesis*, The University of Western Ontario, 2016, http://ir.lib.uwo.ca/etd/3736/.
179 D. Fatta-Kassinos, M. Vasquez and K. Kümmerer, *Chemosphere*, 2011, **85**, 693–709.
180 M. Stylidi, D. I. Kondarides and X. E. Verykios, *Appl. Catal., B*, 2003, **40**, 271–286.
181 A. Houas, H. Lachheb, M. Ksibi, E. Elaloui, C. Guillard and J.-M. Herrmann, *Appl. Catal., B*, 2001, **31**, 145–157.
182 D. Chen and A. K. Ray, *Water Res.*, 1998, **32**, 3223–3234.
183 I. K. Konstantinou and T. A. Albanis, *Appl. Catal., B*, 2004, **49**, 1–14.
184 C. Minero and D. Vione, *Appl. Catal., B*, 2006, **67**, 257–269.
185 J. E. Valladares, *et al.*, Study of haemostatic disorders in experimentally induced leishmaniasis in Beagle dogs, *Res. Vet. Sci.*, 1998, **64**(3), 195–198.